Acta Biomaterialia xxx (xxxx) xxx

Contents lists available at ScienceDirect

Acta Biomaterialia

journal homepage: www.elsevier.com/locate/actbio

Review article

Ion-doped Brushite Cements for Bone Regeneration

K. Hurle[a,*], J.M. Oliveira[b,c], R.L. Reis[b,c], S. Pina[b,c,1,*], F. Goetz-Neunhoeffer[a,1]

[a] GeoZentrum Nordbayern, Mineralogy, Friedrich-Alexander University of Erlangen-Nürnberg (FAU), 91054 Erlangen, Germany
[b] 3B's Research Group, I3Bs – Research Institute on Biomaterials, Biodegradables and Biomimetics, University of Minho, Headquarters of the European Institute of Excellence on Tissue Engineering and Regenerative Medicine, AvePark, Parque de Ciência e Tecnologia, Zona Industrial da Gandra, 4805-017 Barco, Guimarães, Portugal
[c] ICVS/3B's–PT Government Associate Laboratory, Braga/Guimarães, Portugal

ARTICLE INFO

Article history:
Received 16 October 2020
Revised 11 December 2020
Accepted 5 January 2021
Available online xxx

Keywords:
Angiogenesis
Brushite
Bone cements
Drug delivery systems
Ionic dopants
Osseointegration
Tissue regeneration
Tissue engineering

ABSTRACT

Decades of research in orthopaedics has culminated in the quest for formidable yet resorbable biomaterials using bioactive materials. Brushite cements most salient features embrace high biocompatibility, bioresorbability, osteoconductivity, self-setting characteristics, handling, and injectability properties. Such type of materials is also effectively applied as drug delivery systems. However, brushite cements possess limited mechanical strength and fast setting times. By means of incorporating bioactive ions, which are incredibly promising in directing cell fate when incorporated within biomaterials, it can yield biomaterials with superior mechanical properties. Therefore, it is a key to develop fine-tuned regenerative medicine therapeutics. A comprehensive overview of the current accomplishments of ion-doped brushite cements for bone tissue repair and regeneration is provided herein. The role of ionic substitution on the cements physicochemical properties, such as structural, setting time, hydration products, injectability, mechanical behaviour and ion release is discussed. Cell-material interactions, osteogenesis, angiogenesis, and antibacterial activity of the ion-doped cements, as well as its potential use as drug delivery carriers are also presented.

1. Introduction

The population ageing and the consequent increase in the incidence of bone diseases (e.g. osteoporosis, osteoarthritis, and osteomyelitis) and trauma related injuries, resulting from primary tumour resection and orthopaedic surgeries (e.g. total joint arthroplasty and implant fixation), have caused a growing demand for bone filling and repair materials [1]. To overcome this multiplicity of pathologies and injuries, the treatments used by orthopaedic surgeons are mainly internal fixation and bone grafts implantation [2,3]. Autogenous grafts (transplant of tissue from one to another part of the body in the same patient) are among the most successful, but they face a number of limitations regarding the poor availability of collected tissue, chronic donor site pain, morbidity, and complications at the site of harvest. Allogeneic grafts (transplant of tissue from one to another patient with a different genotype) and xenografts (transplant of tissue from donors of another species) also have several drawbacks, among which the risk of immune-mediated rejection and infectious disease transmission.

Given the risks of infection and contamination from the natural origin materials, the discovery of synthetic materials as calcium phosphate-based cements (CPCs) has opened a new era in the medical field of bone grafting [4]. This type of biomaterials is known for its outstanding biocompatibility, resorbability, osteoconductivity, moldability and injectability, and complete filling of any defect geometry [1]. Currently, several CPCs formulations are available for clinical practice as shown in Table 1 [5].

According to their final hydration product, CPCs can be classified as apatite and brushite cements [6]. Apatite formation occurs at pH > 4.2, while brushite precipitates at more acidic conditions at pH < 4.2, at 37 °C [7,8]. Brushite cements were obtained by Mirtchi et al. [9] in 1989, by mixing β-tricalcium phosphate ($Ca_3(PO_4)_2$, β-TCP) and monocalcium phosphate monohydrate ($Ca(H_2PO_4)_2{\cdot}H_2O$, MCPM). These cements have faster setting times and higher resorbability, under physiological conditions, than apatite cements. Brushite is degraded by simple chemical dissolution, while degradation of apatite requires osteoclast activity [10].

* Correspondence authors.
E-mail addresses: katrin.hurle@fau.de (K. Hurle), sandra.pina@i3bs.uminho.pt (S. Pina).
[1] Senior authors.

https://doi.org/10.1016/j.actbio.2021.01.004

Table 1
Commercially available CPCs for orthopaedics applications [5].

Company	Product	Composition	End product
Produits Dentaires SA (CH)	VitalOs	β-TCP, $Na_2H_2P_2O_7$ MCPM, $CaSO_4{\cdot}2H_2O$	Brushite
Synthes (US)	ChronOS Inject®	73 wt% β-TCP, 21 wt% MCPM, 5 wt% $MgHPO_4{\cdot}3H_2O$, < 1 wt% $MgSO_4$, < 1 wt% $Na_2H_2P_2O_7$	Brushite
ETEX (US)	α-BSM®	50 wt% ACP, 50 wt% DCPD	Apatite
	beta-BSM®	n.d.	
	CarriGen	CaPs, sodium carboxymethylcellulose, and sodium carbonate	
	OssiPro	n.d.	
Mitsubishi Materials (JP)	Biopex	α-TCP, TTCP, DCPD	Apatite
Stryker (US)	BoneSource™	73 wt% TTCP, 27 wt% DCPD	Apatite
	HydroSet™	DCPD, TTCP, Trisodium citrate	
BerKeley Advanced Biomaterials (US)	Cem-Ostetic™	n.d.	Apatite
	Tri-Ostetic™	n.d.	
Rebone Biomaterials (CHN)	Rebone	TTCP, DCPA	Apatite
Skeletal Kinetics (US)	Callos™	α-TCP, $CaCO_3$, MCPM	Apatite
	Callos Inject™	α-TCP	
	OsteoVation EX Inject	n.d.	
Biomet (US)	Calcibon®	61 wt% α-TCP, 26 wt% DCPA, 10 wt% $CaCO_3$, 3 wt% CDHA	Apatite
	Biocement D	α-TCP, DCP, $CaCO_3$, PHA	Apatite
Synthes (US)	Norian SRS®	85 wt% α-TCP, 12 wt% $CaCO_3$, 3 wt% MCPM	Apatite
	Norian CRS®		
Lorenz Surgical (GER)	Mimix™	α-TCP, TTCP, HA, citric acid	Apatite
Calcitec (US)	Osteofix	CaPs, CaO	Apatite
Teknimed (FR)	Cementek	TTCP, α-TCP, sodium glycerophosphate	Apatite
	Cementek LV	TTCP, α-TCP, sodium glycerophosphate, dimethylsyloxane	

ACP: Amorphous calcium phosphate; CaPs: calcium phosphates; DCPA: dicalcium phosphate anhydrate; DCPD: dicalcium phosphate dihydrate; MCPM: monocalcium phosphate monohydrate; PHA: precipitated hydroxyapatite; TCP: tricalcium phosphate; TTCP: tetracalcium phosphate; n.d. not defined.

Therefore, brushite cements are of special interest for applications where replacement of the cement by newly forming bone is desired. In contrast, apatite cements have better mechanical strength than brushite cements [5].

It is well known that the presence of bioactive ions (e.g., Mg^{2+}, Sr^{2+}, Zn^{2+}, Mn^{2+}, Cu^{2+}, Li^{+}, Co^{2+}, Cr^{3+}, and Ag^{+}), into the structure of calcium phosphates (CaPs) plays an essential part during the biological action course of the final CPCs, as well as their final mechanical properties [11,12]. Mg^{2+} was shown to prevent risk factors for osteoporosis and can induce angiogenesis [13,14]. Sr^{2+} is reported to inhibit bone degeneration and promote bone formation and it is also medically applied for the treatment of osteoporosis in the form of strontium ranelate [15,16]. Zn^{2+} is able to stimulate osteoblast cell proliferation and differentiation and it also has osteogenesis effects [12]. Mn^{2+} influences the regulation of bone remodelling and its deficit causes reduction of organic matrix synthesis and osteogenesis delays, thus increasing the possibility of bone anomalies such as decreased bone thickness or length [12]. Cu^{2+} is essential in new blood vessels formation and embryonic development, and it is also involved in the generation of reactive oxygen species (ROS) [12,17]. Li^{+} inhibits the negative regulator of Wnt (Wingless-related integration site denotes genes belonging to the INT1/Wingless family) signalling pathway and activates β-catenin-medicated T cell factor occurring in bone and cartilage repair [12]. Co^{2+} and Cr^{3+} doping have shown positive effects on human mesenchymal stromal cells (hMSCs) proliferation and osteogenic differentiation [18]. Co^{2+} can increase bone resorbing osteoclast differentiation [19]. Ag^{+} is well known for its antimicrobial properties against large number of bacteria and toxicity against mammalian cells [20]. Fe^{3+} was reported to promote osteoinduction and new bone formation, and to be effective in reducing cancer cell population by application of magnetic-filed-induced heating [21].

Currently, significant advances on ion-doped brushite cements research have proved the high interest of these biomaterials to the scientific community in bone tissue regeneration/repair. This review presents the last six years´achievements in this field. The role of ionic substitution on the final cements physicochemical properties, namely structure, setting time, hydration products, injectability, mechanical behaviour and ion release are discussed (Table 2). Cell-material interactions, osteogenesis, angiogenesis and antibacterial activity of the doped brushite cements, as well as their potential as drug/biomolecules carriers are also presented (Table 3).

Brushite or dicalcium phosphate dihydrate ($CaHPO_4{\cdot}2H_2O$, DCPD) is a very well crystalline mineral phase with CaPs chains arranged parallel to each other and linked by water molecules (Fig. 1 A) [44]. The first description of a brushite cement was reported by Mirtchi and Lemaitre in 1987 [9], through the reaction of β-TCP and MCPM, resulting in the formation of brushite according to Equation (1) [45].

$$\beta\text{-}Ca_3(PO_4)_2 + Ca(H_2PO_4)_2{\cdot}H_2O + 7\ H_2O \rightarrow 4\ CaHPO_4{\cdot}2H_2O \quad (1)$$

The setting reaction starts by the dissolution of the acidic MCPM in deionized water, which results in a rapid decrease of pH of the cement paste down to a value of 2.5 [46]. This pH drop results in an increase of β-TCP dissolution, which is then followed by brushite crystallization (Fig. 1 B). Bohner et al. [47] thoroughly investigated the hydration of brushite cements with varying β-TCP/MCPM ratio by isothermal calorimetry. Since they did not detect an endothermic peak at early stages in the calorimetry curves of all systems except for pure MCPM and one with very high MCPM excess, they concluded that the reactions must occur simultaneously, resulting in an exothermic peak. This dissolution reaction was followed by the exothermic precipitation of brushite [47]. Detailed investigations of the hydration process of a brushite cement during the first seconds and minutes were further reported by Luo et al. [48] using *in-situ* synchrotron powder X-ray diffraction (XRD). They observed a four-step process for the initial reaction, described as an initial fast reactant dissolution and nucleation induction period followed by nucleation of brushite crystals, a rapid brushite crystal growth period and a slow growth period, where the growth rate of brushite crystals gradually dropped to zero.

Another approach to obtain brushite cements is through the addition of phosphoric acid (H_3PO_4) to β-TCP [49]. The reaction proceeds according to Equation (2).

Table 2
The last six years´achievements of the role of dopant ions on the final physicochemical properties of brushite cements, namely on the setting time, injectability, mechanical strength and ion release [22-35].

Dopant ion in brushite cements	Setting time	Injectability	Mechanical properties	Ion release
Ag^{+}	Increase of setting time with increasing Ag^{+} content, from 3 min for the reference to 7 min for 1.0 wt% Ag^{+} [22]	Not reported	Increase of CS by 30 % for 1 mol% [35]; CS of 4.0 ± 1.0 MPa for 0.6 wt% Ag^{+} and 1.5 ± 1.0 MPa for 1wt% Ag^{+} [22]	Release of 25 µg/L for 0.6 wt% Ag^{+} and 43 µg/L for 1.0 wt% Ag^{+} [22]
Mg^{2+}	IST and FST increased with increasing Mg^{2+} content. FST=4 min for the undoped cement, and 33 min for Mg/(Mg+Ca) = 0.1 [24]; FST increased for 13.3 mol% Mg^{2+}[23]	77 % injectability for Mg/(Mg+Ca) = 0.1 [24]	Decreased microhardness for contents up to 26.67 mol% [23]; Increased CS for higher contents [24]	Initial burst release for 26.67 mol% Mg^{2+} and low release for 66.67 mol% Mg^{2+} [23]
Sr^{2+}	IST and FST increase for Sr^{2+} concentrations up to 6.6 wt% (IST=21 min and FST=25 min [26]; Increase of IST for Sr^{2+}/Mn^{2+} co-doped cements (5 mol% Sr^{2+}≈5 min; 5 mol% Sr^{2+}/0.3 mol% Mn^{2+}≈7.2 min; 5 mol% Sr^{2+}/0.7 mol% Mn^{2+}≈7 min) [25]	66% injectability for 6.6 wt% Sr^{2+} [26]; Injectability ~4% for 5 mol% Sr, and ~97% for 5 mol% Sr containing saccharides in the setting liquid [25]	CS increase from 1.32 to 34 MPa for 6.6 wt% Sr^{2+} content [26]; High strength (CS ≈ 17 MPa) was obtained for cement containing 0.32 mol% Mn and 5 mol% Sr, prepared with sucrose as additive [25]	Release of 17.2 % of Sr into MG63 culture medium, from cements containing 5 mol% Sr^{2+} [25]
Zn^{2+}	Increase of IST and FST for 0.25 wt% Zn^{2+} [32]; Increase of setting time: 7 min for undoped sample, 13 min for 0.6 wt% Zn^{2+} and 19 min for 1.2 wt% Zn^{2+} [30]	The required force for unit displacement was higher for 6 wt% Zn/15 wt% Si and 9 wt% Zn/15 wt% Si, and lower for 3 wt% Zn/15 wt% Si (tested in an universal testing machine with a crosshead of 0.5 mm/min) [34]	Decrease of CS for 0.25 wt% Zn^{2+} content [32]	Release of 0.30 ± 0.01 for 0.6 wt% and 0.10 ± 0.01 µg/L for 1.2 wt% content [30]
Mn^{2+}	Increase of IST for Sr^{2+}/Mn^{2+} co-doped cements (5 mol% Sr^{2+}≈5 min; 5 mol% Sr^{2+}/0.3 mol% Mn^{2+}≈7.2 min; 5 mol% Sr^{2+}/0.7 mol% Mn^{2+}≈7 min) [25]	Injectability of ~80% for 0.5 and 1 mol% Mn content, and 100% injectability when saccharides were incorporated in the setting liquid [25]	High strength (CS ≈ 17 MPa) was obtained for cement containing 0.32 mol% Mn and 5 mol% Sr, prepared with sucrose as additive [25]; Decrease of CS with the increase of Mn content, from 19.71 ± 2.45 MPa for undoped cements and 11.70 ± 1.16 MPa for cements containing 30 wt% Mn-TCP [33]	Higher initial Mn amounts (0.7 mol%) released a higher Mn amount (~0.4 mg g^{-1}) [25]
Co^{2+}	Decrease of IST=2.21 ± 0.04 min for 0.3 wt% Co^{2+}, and increase of IST=6.80±0.08 min for 1.2 wt% Co^{2+} [28]	Not reported	CS reduction from 3.17 ± 1.04 MPa to 1.09 ± 0.21 MPa for 1.2 wt% content [28]	Initial release was up to tenfold higher compared to the release after 16 days of cultivation. Released Co^{2+} after 1 day of incubation, of 247 ± 26 μM [19]
Cu^{2+}	Increase of the setting time=50 min for 5% Cu content [31]	88% injectability for 5% Cu [31]	Decrease of CS for 50 mmol content [18]	Initial burst release for 10 and 50 mmol Cu^{2} [18]; Released Cu^{2+} after 1 day of incubation of 305 ± 23 μM, which is above the cytotoxic threshold for osteoclasts (~30 μM) [19]
Cr^{3+}	Not reported	Not reported	Decrease of CS for 50 mmol content [18]	Very low amount release during cell cultivation [19]
Fe^{3+}	Increase of setting time up to 123 min for 5 mol% Fe^{2+} [27]	Not reported	High CS for 0.49 wt% Fe^{3+} content [21]	Fe released in physiological media from 0.49 wt% Fe^{3+}, after 10 days, within the range of clinically acceptable Fe blood levels [21]
Si^{4+}	Increase of FST=19 min for 1.1 wt% Si^{4+} and no significant effect for 0.5 wt% Si^{4+} [29]	The required force for unit displacement was higher for 6 wt% Zn/15 wt% Si and 9 wt% Zn/15 wt% Si, and lower for 3 wt% Zn/15 wt% Si (tested in an universal testing machine with a crosshead of 0.5 mm/min) [34]	CS of 4.32±0.63 MPa for 0.5 wt% Si content [32]	SiO_4^{4-} ions release of 33 and 38 ppm respectively, from 40% Si-CPC and 80% Si-CPC, after 3 days immersion in double-distilled water [81]

CS: compressive strength; FST: final setting time; IST: initial setting time.

Table 3
The last six years´achievements of the role of dopant ions on the final biological properties of brushite cements, namely on cell viability/proliferation, osteoclast activity, osteogenesis/angiogenesis, antibacterial studies and its use as drug/biomolecules delivery systems [18,19,21-26,28-33,35-43].

Dopant ion in brushite cements	Cell viability and proliferation	Osteoclast activity/in vivo biodegradation	Osteogenesis /Angiogenesis	Antibacterial activity	Drug/Biomolecules delivery systems
Ag^{+}	Low toxicity of human adipose-derived stem cells growth on 10 mol% Ag^{+} [36]	Not reported	Not reported	Decrease of *S. aureus* adhesion and an inhibitory effect towards pathogenic *E. coli* for Ag^{+} amounts of 0.6 and 1 wt% [22,35]	Not reported
Mg^{2+}	Increased cell proliferation in the Mg-doped cements in comparison without Mg [41]	Progressive degradation of the cements after 8 weeks of implantation in rabbits [41]	New bone formation with complete defect filling for all compositions, 6.67 % Mg-CPC, 26.67 % Mg-CPC and 40 % Mg-CPC [41]	Not reported	The drug release was shown to be fast for 26.67 mol. % Mg^{2+} and slow for higher Mg^{2+} concentrations [41]; A burst release of gentamicin sulfate, amoxicillin and ampicillin trihydrate in the first 12 hours [24]
Sr^{2+}	High cell proliferation and differentiation for 5 mol% Sr^{2+} [25]	Not reported	Complete filling of bone defect for 5 wt% Sr^{2+} [37]	Not reported	Increased drug release observed in the first 72 hours for 6.6 wt% Sr^{2+} content, of 96 %, 87 % and 73 %, respectively for gentamicin sulfate, amoxicillin, and ampicillin trihydrate [26]
Zn^{2+}	High ALP activity in MG63 cells [43]	Osteoclast activity after 14 days cultivation of MG63 cells [43]	Moderate bone regeneration for 0.25 wt. % Zn combined with 0.5 wt. % Si [32]; Increased angiogenic potential [43]	Inhibitory effect towards *E. coli* for 0.6 wt% Zn^{2+} [30]	Improved new bone formation of IGF-1 loaded 0.25 wt% Zn-doped cements [32]
Mn^{2+}	High cell proliferation and differentiation for 0.32 mol% Mn^{2+} [25]; Inhibition of mBMSCs proliferation after 3 days culture, for Mn^{2+} concentration greater than 28.21 μg/L [33]	Not reported	Addition of 10 wt% Mn-TCP induced the G1 arrest in mBMSCs and simulated the osteogenesis-related gene expression [33]	Not reported	Not reported
Co^{2+}	High cell proliferation for Co^{2+} concentration $\leq$ 50 μM, while 250 μM showed reduced cell proliferation [18]	Osteoclast cells detected on cements with 10 mmol Co, after 16 days of cultivation [19]	Not reported	Not reported	Not reported
Cu^{2+}	Dose range of 1 – 2.5 mg/mL showed positive proliferative effect on human glial E297, murine osteoblastic K7M2 and human primary lung fibroblasts cells [38]; Cu^{2+} concentrations $\leq$ 100 μM resulted in enhanced proliferation of hMSCs [18]	After 16 days of cultivation, no osteoclast-specific enzymes TRAP, CAII and CTSK, were detected in 10 mmol Cu^{2+}, and Cu^{2+} at 18 μM completely inhibited resorption [19]	Not reported	Antibacterial effects against *E. coli, P. aeruginosa and S. enteritidis* for Cu^{2+} content of 0.3 wt% [38]; Larger inhibition zones of *E. coli*, *S. aureus*, and *P. aeruginosa* with increasing Cu content, and prominent inhibition halos produced toward *P. aeruginosa* [31]	Not reported
Cr^{3+}	High cell proliferation for 50 mmol Cr^{3+} [18]	High osteoclast activity for 50 mmol Cr^{3+} [39]; Osteoclast cells detected on cements with 10 mmol and 50 mmol Cr^{3+}, after 16 days of cultivation [19]	Osteogenic differentiation for 50 mmol Cr^{3+} [39]	Not reported	Not reported
Fe^{3+}	High cellular activity for Fe^{3+} content up to 0.50 wt% [21,40]	Not reported	High levels of osteocalcin and Runx2 in MC3T3-E1 cells for 0.49 wt% and 1.09 wt% Fe^{3+} [21]	Antibacterials activity against *E. coli, S. enteritidis, P. aeruginosa*, and *S. aureus* [21]	Not reported
Si^{4+}	High ALP activity in MG63 cells [43]	High TRAP activity for 0.5 wt% Si^{4+} [29]	Fast neoosseous formation and vasculogenesis enhancement, for high (0.5, 0.8, and 1.1 wt%) Si^{4+}amounts [29,32]; Increased angiogenic potential [43]	Not reported	Release of 98 % of vancomycin in 80 % [Si/(Si+P)] content, after 168 hours [42]; Improved new bone formation of IGF-1 loaded 0.5 wt% Si-doped cements [32]

ALP: alkaline phosphatase; CAII: carbonic anhydrase II; CTSK: cathepsin K; mBMSCs: mouse primary bone marrow-derived mesenchymal stem cells; hMSCs: human mesenchymal stromal cells; IGF: insulin-like growth factor; TRAP: tartrate-resistant acid phosphatase.

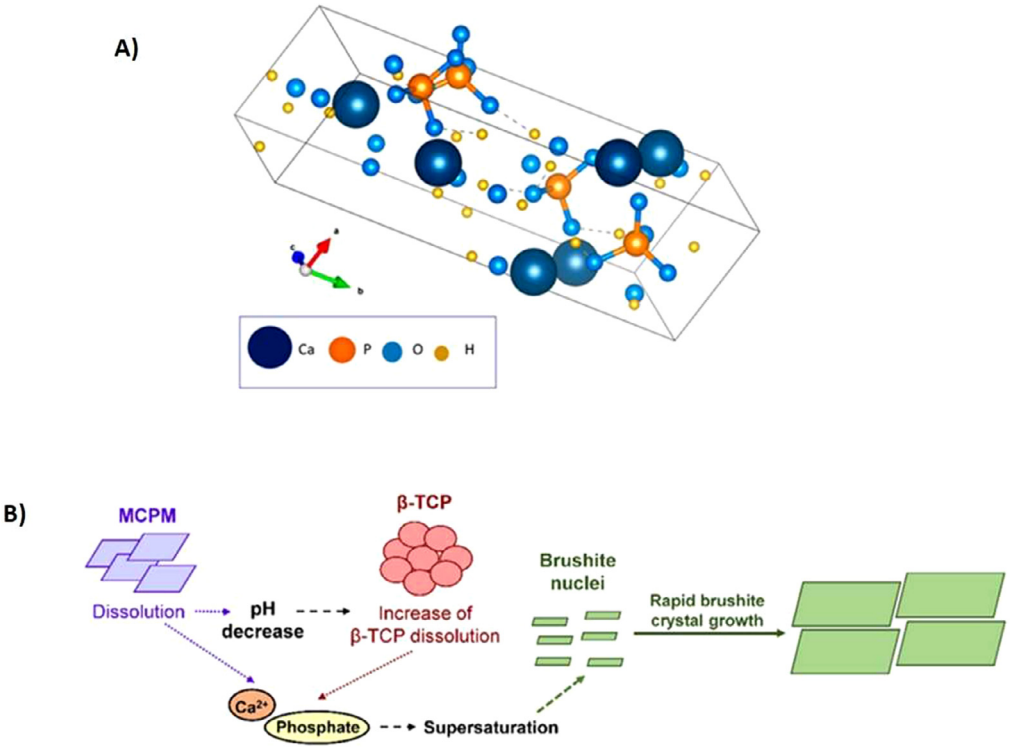

Fig. 1. Schematic representation of: A) Crystalline structure of brushite. Reprinted from [44]; and B) Schematic representation of brushite formation.

$$Ca_3(PO_4)_2 + H_3PO_4 + 6H_2O \rightarrow 3CaHPO_4{\cdot}2H_2O \quad (2)$$

Regarding a successful clinical application of the cements, several properties need to be considered and carefully adjusted, namely the setting time, injectability, dynamic of flow, mechanical properties and the resorption rate. The main important factor is the setting time. While hardening needs to be slow enough to give the surgeon time for implementation of the cement, a too slow hardening time would unnecessarily delay the operation. Therefore, the ideal setting time would be in the range of a few minutes [50]. Another relevant aspect is the injectability of the cement paste for minimal-invasive applications, where the cement is directly inserted into the defect through a syringe with narrow cannulas. Several approaches were developed to improve the injectability of the cement pastes, namely by adjusting particle sizes to a bimodal distribution [51] or using additives, such as citric acid [52,53] or phytic acid [54,55], that alter the zeta potential of the particles surface and therefore increase the particle repulsion. In addition to their fluidizing effect, sulphate, pyrophosphate, citrate and phytic acid have also been used as retarding agents in brushite cements [53,54,56,57]. For example, Hurle et al. [54] studied the effect of phytic acid as a setting regulator, compared with citric acid, in brushite cements. An improvement on the injectability and an increased reaction delay for higher phytic acid amounts was shown. Besides, it was observed that even small phytic acid concentrations were enough to adjust favourable setting and rheology performances.

The rheological properties have another crucial importance in gaining understanding of the fundamentals of the dynamics of flow of an injectable CPC, through the delivery system (cannula) and its subsequent interdigitating into the trabecular bone [58]. In general, CPCs are considered viscoelastic materials since they change from primarily liquid-like properties immediately after mixing to primarily solid-like properties once cured. The mechanical behaviour of the cements is of paramount importance, as a compressive strength close to 10-12 MPa comparable to that of trabecular bone is required. In general, all factors that influence the injectability also influence the strength of the cements. Thus, the characteristics of the starting powders, such as particle size, the proportion and nature of the hydrate phases formed, the liquid-to-powder ratio (LPR), and the presence (and/or variation) of additives can significantly change the strength of the materials [59].

1.1. Ion doping into the structure of β-TCP

Tricalcium phosphate (TCP) exists in two different modifications that are relevant for application. While α-TCP is stable at temperatures above 1125 °C and can be stabilized at room temperature by quenching, β-TCP forms at lower temperatures [60]. The different crystal structures of both phases result in different solubility and hydraulic activity. The α-TCP shows hydraulic activity in its crystalline form, while crystalline β-TCP is hardly soluble in water [61]. Still, it can be rapidly dissolved in the acidic environment of brushite cements, which results in their rapid hardening.

β-TCP is rhombohedral with the space group R3c. The structure can be described as consisting of two different columns aligned parallel to the crystallographic *c* axis [62]. The columns altogether contain five different Ca^{2+} positions. The coordination of the Ca^{2+} ion on the five positions with oxygen is sevenfold, eightfold, eightfold, fourfold and sixfold, respectively (Fig. 2). While the occupancy of the Ca(4) position is 0.43(4), all other positions are fully occupied [63].

In the β-TCP structure, different ions can be incorporated in the Ca^{2+} positions. The dopant ions can preferably substitute Ca^{2+} on certain atomic positions, depending on their ionic radii for the relevant coordination with oxygen.

Mg^{2+} was shown to incorporate into the structure of β-TCP up to a concentration of 14 mol% preferably occurring on the Ca(5) site [65]. After complete occupation of this site, the Ca(4) site is then occupied. Due to smaller ionic radius of Mg^{2+}, compared to Ca^{2+} (0.720 and 1.00 Å, respectively, both given for sixfold coordination [66]), the incorporation of Mg^{2+} results in a decrease of

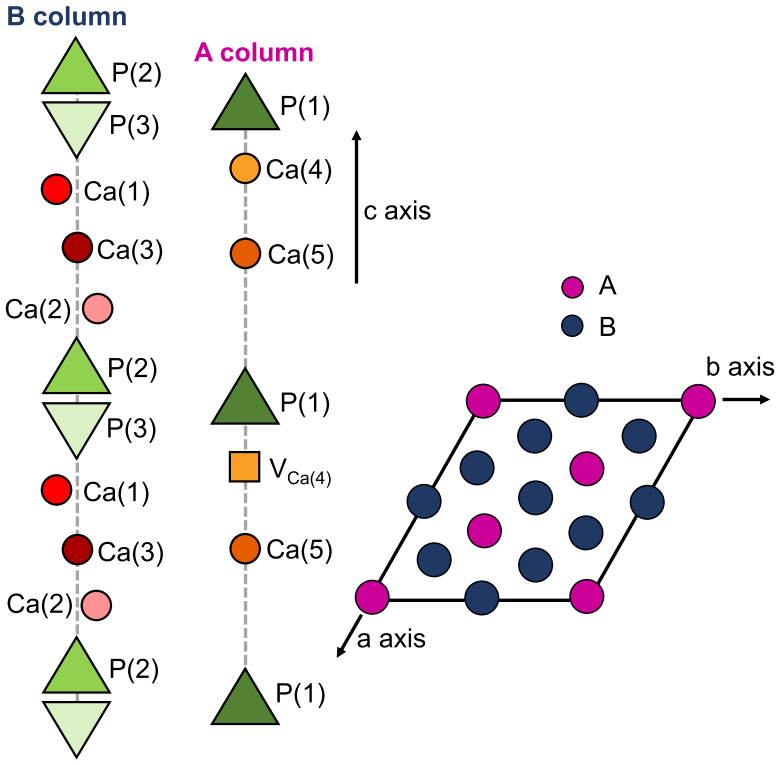

Fig. 2. Schematic representation of the β-TCP structure based on Yoshida et al. [64].

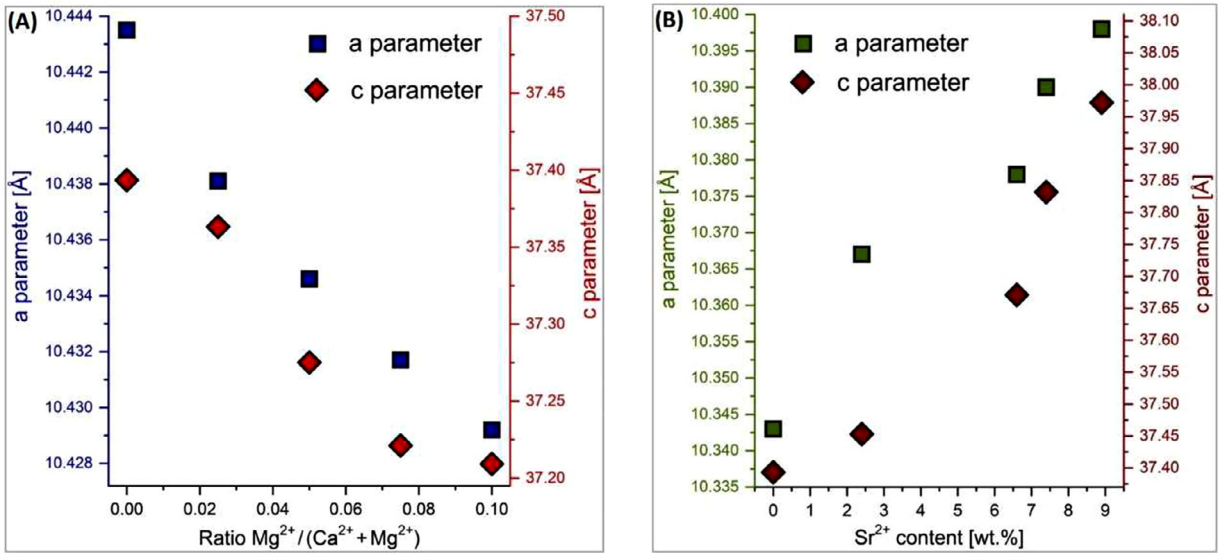

Fig. 3. Diagrams of the β-TCP lattice parameters *a* and *c* with increasing content of Mg^{2+} (A) [24], and Sr^{2+} (B) [68].

the β-TCP lattice parameters *a* and *c* (Fig. 3 A). Substitution of Sr^{2+} into the β-TCP structure can occur over a wide range of compositions [67]. As a result of its higher ionic radius compared to Ca^{2+} (1.18 Å and 1.00 Å, respectively, for sixfold coordination [66]), an increase of both parameters is observed (Fig. 3 B).

Different studies were reported dealing with the incorporation of Cu^{2+} into β-TCP. While these studies agreed that Cu^{2+} mainly occupies the Ca(5) position in the β-TCP structure, the data differ in their reported substitution limits. Nord [69] reported a substitution limit of 12 mol%. In contrast, Matsumoto et al. [70] set the limit for Cu^{2+} incorporation of 9.09 mol% for β-TCP co-doped with Ag^{+} and Cu^{2+}. This substitution limit reached a full occupancy of the Ca(5) positions by Cu^{2+}, while the Ag^{+} fully occupies the Ca(4) position up to a limit of 9.09 mol%. A recent study by Spaeth et al. [71] proposed an incorporation limit between 14 and 15 mol% Cu^{2+} in the structure of β-TCP, as a Cu^{2+} containing secondary phase started to form at a content of 15 mol%. Furthermore, a clear decrease of both lattice parameters *a* and *c* with increasing Cu^{2+} content was observed (ionic radius for Cu^{2+}: 0.73 Å, for sixfold coordination [66]) (Fig. 4 A).

Different authors have found that the substitution limit for Ag^{+} in β-TCP is in the range of 8 - 10 mol%, as the secondary phase Ag_3PO_4 was reported for 10 mol% Ag^{+} content [73,74]. This substitution resulted in a decrease of the *c* parameter, while the *a* pa-

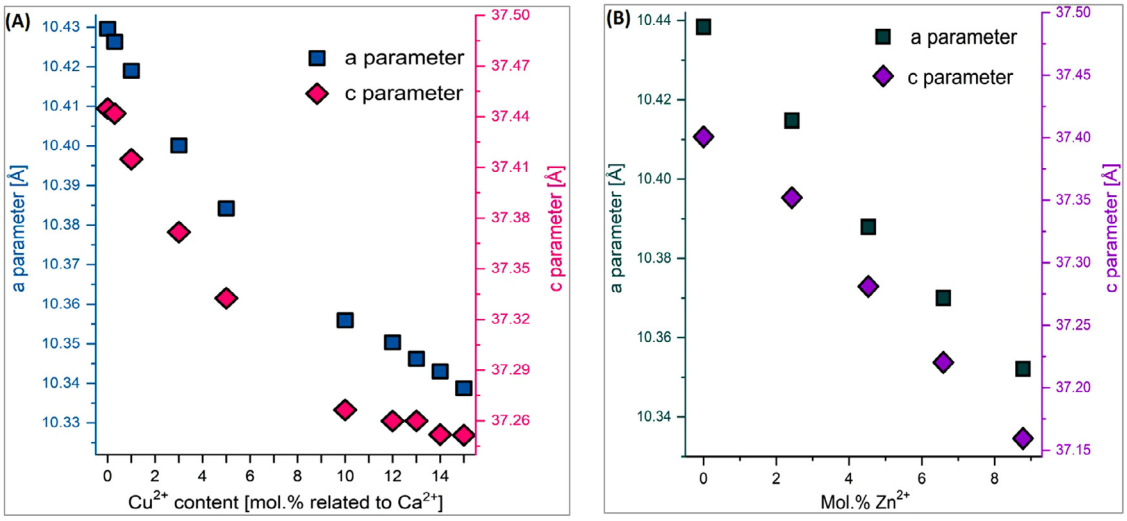

Fig. 4. Diagrams of the β-TCP lattice parameters *a* and *c* with increasing content of Cu^{2+} (A) [71] or Zn^{2+} (B) [72].

rameter remained constant. They further suggested that the substitution occurred by replacing one vacancy and one Ca^{2+} ion at the Ca(4) position by two Ag^{+} ions, but with no proof of this theory.

Similarly, different substitutions of Zn^{2+} are reported. Matsumoto et al. [70] showed a limit of 9.09 mol% Zn^{2+}, which was incorporated at the Ca(5) position. In contrast, Gomes et al. [75] proposed the substitution at both Ca(4) and Ca(5) position, which resulted in a substitution limit of 13.6 mol% Zn^{2+} [64]. In accordance to Mg^{2+} and Cu^{2+}, Zn^{2+} incorporation (Zn^{2+} ionic radius: 0.740 Å, for sixfold coordination [66]) results in a reduction of both the *a* and *c* parameter (Fig. 4 B).

1.2. Physicochemical properties of ion-doped brushite cements

1.2.1. Setting time / setting reaction

Ionic dopants move to the mixing liquid upon dissolution of the CPCs and can thus significantly influence the setting time [36,40,76]. Owing to its importance for the clinical application, the setting time needs to be fully investigated for the development of functional brushite cement formulations incorporating dopants ions.

The Mg^{2+} role on the setting behaviour of a brushite cement was studied by several authors. Saleh et al. [24] studied the setting of brushite cements composed of MCPM and β-TCP doped with different Mg^{2+} concentrations (Mg/(Mg+Ca) molar ratios of 0, 0.025, 0.05, 0.075 and 0.1). They showed that both initial (IST) and final setting time (FST) were remarkably increased with increasing Mg^{2+} content. FST was 4 min for the undoped cement and increased up to 33 min for the sample with Mg/(Mg+Ca) = 0.1. Alkhraisat et al. [23] investigated cements containing monocalcium phosphate (MCP) and powders with a Mg/(Mg+Ca) molar ratio up to 66.67% composed of Mg^{2+}-substituted β-TCP, stanfieldite ($Ca_4Mg_5(PO_4)_6$) and/or farringtonite ($Mg_3(PO_4)_2$). In the same manner, Saleh et al. [24] observed an increase of FST by Mg^{2+} incorporation up to 13.3 mol%. The setting time decreased for higher Mg^{2+} concentrations, attributed to the formation of newberyite ($MgHPO_4{\cdot}3H_2O$) in addition to brushite.

Taha et al. [26] analyzed brushite cements composed of β-TCP doped with different Sr^{2+} concentrations (0, 2.4, 6.6, 7.4 and 8.9 wt%) and MCPM. They observed a significant increase of both IST and FST for Sr^{2+} concentrations up to 6.6 wt% (IST: 2 min for reference, 21 min for 6.6 wt% Sr^{2+}; FST: 4 min for reference, 25 min for 6.6 wt% Sr^{2+}). The setting times decreased for higher Sr^{2+} concentrations due to monetite formation, but still above the values obtained for the undoped samples.

The setting of brushite cements containing β-TCP co-doped with Mn^{2+} and Sr^{2+} (Sr^{2+} concentration: 5 mol%; Mn^{2+} concentration: 0, 0.3 and 0.7 mol%) was investigated by Torres et al. [25]. They observed an increase of IST for both Sr^{2+}-doped and Sr^{2+}/Mn^{2+} co-doped samples, being more pronounced for the co-doped samples (reference $\approx$ 2.8 min; 5 mol% Sr^{2+} $\approx$ 5 min; 5 mol% Sr^{2+} + 0.3 mol% Mn^{2+} $\approx$ 7.2 min; 5 mol% Sr^{2+} + 0.7 mol% Mn^{2+} $\approx$ 7 min). An increase by a factor of more than 2.5 was observed for the samples containing 5 mol% Sr^{2+} and 0.7 mol% Mn^{2+}, compared to the undoped reference. This was explained by a synergistic effect resulting from the presence of both ions, leading to the enhancement of the chemical stability towards the setting liquid.

Similarly, an increase of the setting time was reported for brushite cement composed of Fe^{2+} doped β-TCP and MCPM with the addition of 1 wt% chitosan by Li et al. [27]. The setting time increased with increasing Fe^{2+} concentration up to 123 min for 5 mol% Fe^{2+}, which was about tenfold compared to the reference (12 min). Furthermore, a decrease of conversion rate after 72 h of setting was indicated by the decrease of brushite reflection intensities with increasing Fe^{2+} content, accompanied by an increase of residual MCPM reflection intensities. $Ca_{19}Fe_2(PO_4)_{14}$ was additionally detected in samples with higher iron content. While no characterization of the starting powder was reported [27], it is logical to assume that this compound was already present in the starting powder [27]. This assumption is supported by the observations of Uskokovic et al. [21], who reported the formation of the similar compound $Ca_9Fe(PO_4)_7$ and small amounts of hematite in β-TCP starting powders doped with 0.49 and 1.09 wt% Fe. Although the effect of Fe^{3+} on the setting time was not reported in this study, as the setting reaction was only investigated by Energy Dispersive X-Ray Diffraction (EDXRD) for one Fe^{3+} concentration, the authors stated that the cement setting was relatively fast.

Vahabzadeh et al. [28] investigated brushite cements containing β-TCP doped with variable Co^{2+} contents (0, 0.3, 0.5 and 1.2 wt%). While the IST of the samples containing 0.3 wt% Co^{2+} decreased from 3.67 $\pm$ 0.23 min (reference) to 2.21 $\pm$ 0.04 min, it increased to 6.80 $\pm$ 0.08 min for 1.2 wt% Co^{2+}. The increase of setting time for higher Co^{2+} concentrations was attributed to a stabilization of the β-TCP structure by incorporation of the smaller Co^{2+} ion compared to Ca^{2+}, resulting in reduced solubility, whereas the decrease of setting time observed for 0.3 wt% Co^{2+} was attributed to the possible formation of $CoHPO_4$ with high solubility. Cummings et al.

[77] reported a reduction of brushite formation with increasing Co^{2+} content on brushite cements containing β-TCP doped with 0.25, 0.5 and 1 wt% Co^{2+} (no secondary phases detected). This fact was attributed to the reduction of β-TCP solubility by lattice shrinkage induced by the smaller Co^{2+} ion [28].

Vahabzadeh et al. [29] investigated the setting of brushite cements containing β-TCP doped with 1.1 wt% Si^{4+}. No impact of Si^{4+} on the IST was observed, and the FST was significantly increased from 11-12 min (undoped reference) to 19 min. Furthermore, no significant effect of Si^{4+} on the setting time of brushite cements containing β-TCP doped with 0.5 wt% Si^{4+}, 0.25 wt% Zn^{2+} or co-doped with 0.5 wt% Si^{4+}/ 0.25 wt% Zn^{2+} was reported [32]. On the other hand, the addition of Zn^{2+} led to a significant increase of the IST and FST, attributed to the stabilization of the β-TCP structure by Zn^{2+}, which retards β-TCP dissolution. The setting times of brushite cements with Zn^{2+}-doped β-TCP were also investigated by Graziani et al [30]. They observed an increase of the setting time with increment of Zn^{2+} content (7 min for undoped sample, 13 min for 0.6 wt% Zn^{2+} and 19 min for 1.2 wt% Zn^{2+}). The setting delay was explained by the formation of $CaZn_2(PO_4)_2$ detected by in-situ time resolved EDXRD measurements, which can hinder brushite crystal growth. In accordance, a lower conversion rate was observed for the Zn^{2+} containing samples.

Ag^{+} did not show any effect on the setting time of a brushite cement composed of β-TCP doped with 1 mol% Ag^{+} and monocalcium phosphate anhydrate [35]. Contrary to this, Rau et al. [22] observed an increase of cement setting time with increasing Ag^{+} content from 3 min for the reference to 7 min for an Ag^{+} content of 1.0 wt%. The cements were obtained by adding magnesium dihydrogen phosphate tetrahydrate with phosphoric acid and 30 wt% glycerol solution with a LPR of 3/4 mL/g. The increased setting time was accompanied by a lower conversion rate for both samples doped with Ag^{+} (0.6 and 1.0 wt% Ag^{+} content). While in [35] no secondary phases were detected in the Ag-doped TCP, in [22] metallic Ag^{+} was detected as secondary phase after sintering the precipitated powders at 1300 °C.

It has to be taken into account that all single data presented above cannot be directly compared with each other. Dissolution rates and consequently setting times in practice are also quite dependent from synthesis temperature, particle fineness, possible further cement additives and LPR.

1.2.2. Hydration products of brushite cements

Ionic dopants have the potential to affect not only the hydration kinetics, but also the hydrate phases which precipitate during hardening. The dopants can be incorporated into the crystal structure of the hydrate phases and alter their crystal morphology. These parameters can then in turn affect the biological performance of the hardened cement.

Li et al. [27] observed larger brushite crystal particles for cements incorporating different concentrations up to 5 mol% of Fe^{2+}, which effect appeared to be independent on the Fe^{2+} content. While a decrease of brushite XRD peak intensity was reported, no information about the development of the lattice parameters was provided. Indeed, indications for Fe^{3+} substitution in brushite were reported by Uskokovic et al. [21] by peak shifts in the corresponding XRD time resolved in-situ spectra in comparison to the reference. In contrast to this, no peak shift was recorded for brushite nanoparticles doped with different Fe^{3+} contents [78]. Still, it was observed an increase of crystallite size determined according to Sherrerś equation with increasing Fe content from 23 to 74 nm (Fig. 5).

Schamel et al. [18] observed no effect of 50 mmol Co^{2+} or Cu^{2+} doped β-TCP on the morphology of brushite. They presented plate-like crystals for both ions, as well as for the undoped reference. In contrast, an effect of doping β-TCP with 50 mmol Cr^{3+} was noticed

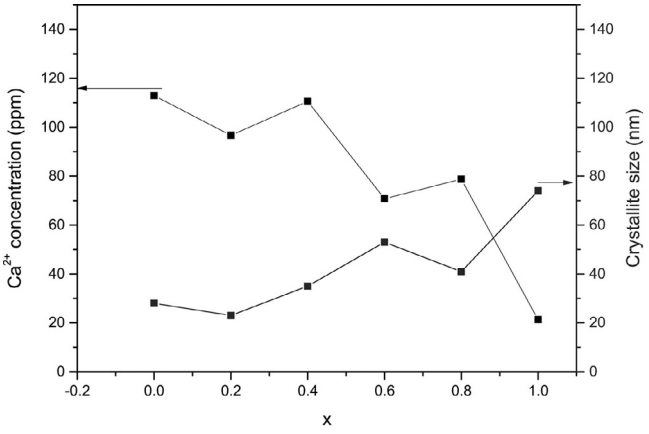

Fig. 5. Dependence of the hydration products crystallite size and Ca^{2+} content on the Fe^{3+} content. Reprinted with permission from [78].

(Fig. 6). Here, agglomerates of small particles in the dimension of the crystals in the other cements were observed. This was accompanied by a change of phase composition. While slight amounts of monetite ($CaHPO_4$) were formed in addition to brushite in all samples, its content was remarkably higher in the sample containing 50 mmol Cr^{3+}.

Co-doping with Si^{4+} and Zn^{2+} can change the brushite crystal morphology from a compact structure (in the undoped cements) to individual needle/plate-like crystals in the cements doped with different ions concentration (0.5 wt% Si^{4+}, 0.25 wt% Zn^{2+} or 0.5 wt% Si^{4+} / 0.25 wt% Zn^{2+}), whereas maintaining the qualitative phase composition [32]. Vahabzadeh et al. [29] observed no effect on the phase composition of the hydrated cement by adding 1.1 wt% Si^{4+}, as only remaining β-TCP and brushite were present. In the study of Graziani et al. [30], a clear effect of Zn^{2+} doping on phase transformations was observed. While in the undoped reference, brushite and residual β-TCP were present after hardening, only monetite was detected in the cements doped with 1.2 wt% Zn^{2+} as hydration product. Furthermore, $CaZn_2(PO_4)_2$ was detected in both Zn^{2+} containing samples (0.6 and 1.2 wt%). Though the authors claimed that this phase was absent in the starting powders, it appears unlikely that this non hydrated phase really formed by precipitation from solution after the mixing liquid addition. Instead, $CaZn_2(PO_4)_2{\cdot}2H_2O$ is formed by precipitation from solution, thus requiring a thermal treatment to remove the structural water and to obtain $CaZn_2(PO_4)_2$ [79]. It is therefore more plausible that the phase was already present in the starting powders, but not detected, and remained unreacted during hydration.

Co-doping with Mn^{2+} and Sr^{2+} (Sr^{2+} concentration: 5 mol%; Mn^{2+} concentration: 0, 0.3 and 0.7 mol%) had nearly no effect on qualitative phase composition [25]. In contrast, Taha et al. [26] found that Sr^{2+} favored the formation of monetite, which appeared as main hydration product for higher Sr^{2+} contents (7.4 and 8.9 wt%). The observed increase of the brushite lattice parameters was indicative of Sr^{2+} incorporation for the cements with lower Sr^{2+} concentrations, while additionally a distortion of the structure of brushite and monetite was evidenced by Fourier Transform Infrared (FTIR). Furthermore, the authors described a change from small structured particles of irregular morphology to loosely packed plate-like morphology with heterogeneous size distribution by Sr^{2+} incorporation.

No influence of 1 mol% Ag^{+} doping on brushite crystal morphology or on its diffraction pattern was observed in [35]. In 1 wt% Ag^{+}-doped cement studied by Rau et al. [22], the formation of divalent calcium-silver polyphosphate $CaAg(PO_3)_3$ was claimed in addition to brushite formation, since this phase was not detected

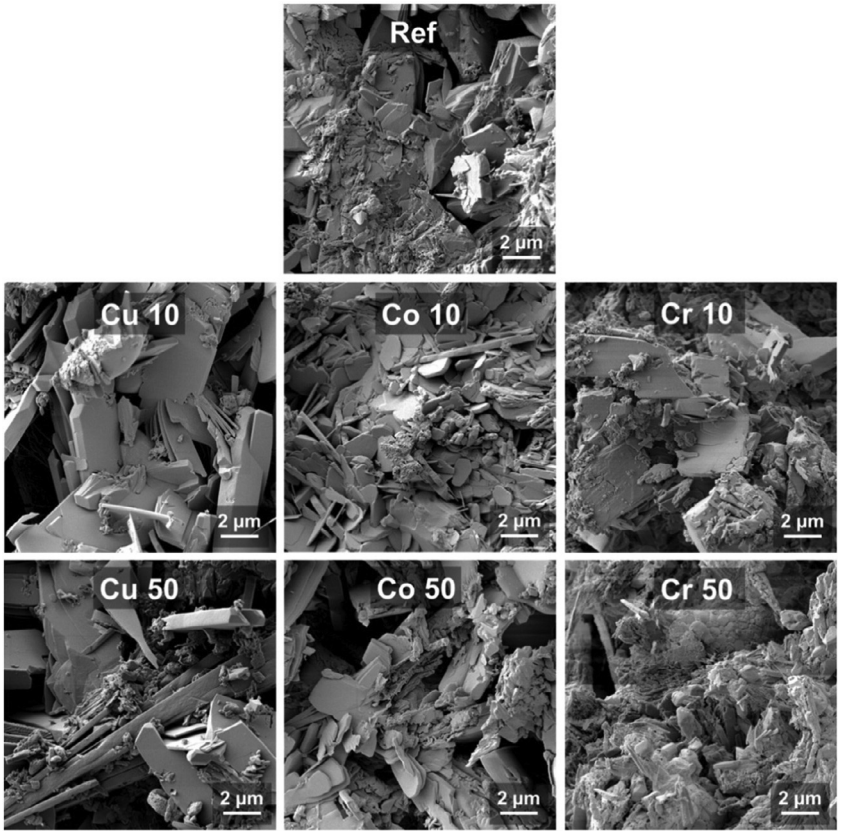

Fig. 6. Microstructure of brushite fractured surfaces obtained by scanning electron microscopy: brushite reference (Ref) and cements doped with 10 mmol Cu^{2+} (Cu 10), 50 mmol Cu^{2+} (Cu 50), 10 mmol Co^{2+} (Co 10), 50 mmol Co^{2+} (Co 50), 10 mmol Cr^{3+} (Cr 10) and 50 mmol Cr^{3+} (Cr 50) per mol β-TCP. Reprinted with permission from [18].

in the starting powders, but in the hydrating cement pastes. The peaks resulting from metallic Ag, which was claimed to be present in the starting powders, were not detected. While these observations indicated a reaction of metallic Ag with Ca^{2+} and PO_4^{3-} ions in solution, resulting in the formation of $CaAg(PO_3)_3$, this appears chemically implausible. The authors did not present any theory or proposed reaction scheme to explain their observations. The morphology of the cements was not noticeably affected by the Ag^{+} addition and the brushite was present in the typical plate-like shape [22].

A clear effect on brushite crystal morphology was also observed for Se^{4+} incorporated into brushite synthesized via wet precipitation method in a concentration of 0.67 wt% [80]. Plate-like crystals with a diameter and length of around 10 µm and 20–30 µm, respectively were obtained for the undoped reference, while the morphology changed to rod-like crystals with a diameter of 5–7 µm and length higher than 25 µm for Se^{4+}-doped samples. Furthermore, Se^{4+} incorporation into the brushite lattice was indicated by change of the lattice parameters, namely a significant increase of *a* parameter and simultaneous decrease of *c* parameter. Furthermore, the substitution of phosphate by selenite SeO_3^{2-} was confirmed by solid state $^{1}H \rightarrow {}^{31}P$ cross-polarization combined with magic-angle spinning (CP MAS) kinetics experiments.

Additional phases can be already present in the β-TCP starting material, if a higher amount of the respective dopant is present. These phases might then react to form hydrate phases other than monetite and brushite. For example, the starting powder of the Mg^{2+} modified cements investigated by Alkhraisat et al. [23] contained stanfieldite and / or farringtonite in addition to Mg^{2+}-doped β-TCP. Consequently, the magnesium phosphate hydrate phase newberyite ($MgHPO_4{\cdot}3H_2O$) was formed in addition to brushite at higher Mg^{2+} contents. Besides, indications of 3 mol% Mg^{2+} incorporation into the structure of brushite were found by application of selected-area electron diffraction (SAED) and Energy Dispersive X-Ray (EDX). Still, no clear tendency of brushite lattice parameters with increasing Mg^{2+} content was observed. Similarly, the incorporation of Mg^{2+} into the brushite structure was indicated by a shift of the XRD peaks, being more pronounced for higher Mg^{2+} contents [24]. However, since no refined lattice parameters were reported for brushite, it cannot be excluded that the observed peak shifts might also result from preparation-related effects. Additionally, the broadening of the FTIR signals representative of the brushite cements (a detailed overview of the brushite IR vibration modes is elsewhere reported [24]) was noticed, which is indicative of the lattice distortion induced by Mg^{2+} incorporation. Mg^{2+} was further shown to favor the formation of larger-sized particles as flake- or needle-like, while an irregular morphology was present in the cements without Mg^{2+} [24]. Newberyite formation in addition to brushite was also observed in the cement system investigated by Cabrejos-Azama [41], which contained starting powders with molar Mg/(Mg+Ca) ratios between 26.67 and 66.67%.

Aparicio et al. [81] developed brushite cements containing Si^{4+}-doped β-TCP with Si^{4+} contents up to 80 mol% Si/(Si+P). It was shown that the phase composition of the hydrated cement was strongly dependent on the Si^{4+} content. Brushite was present in all samples (mainly in those with Si^{4+} contents up to 60 mol%) and silicocarnotite ($Ca_5(PO_4)_2SiO_4$) in the doped samples, while the sample with the highest Si^{4+} content was mainly composed of an amorphous phase. No XRD analyses of the sintered powders were reported, but for logical reasons it can be assumed that the silicocarnotite was not formed during hydration, but was already present in the sintered starting powders. Furthermore, HAp was present as hydration product in the Si^{4+} containing samples. Cement morphology was affected by the Si^{4+} content by observing

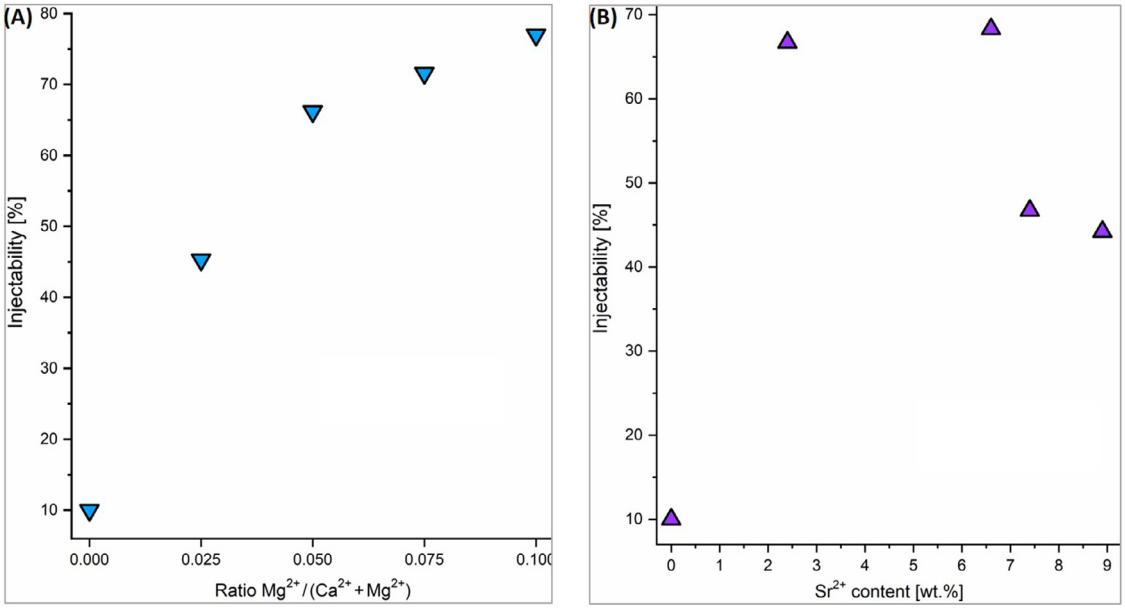

Fig. 7. Influence of ionic doping with Mg^{2+} (A) [24] and Sr^{2+} (B) [26] on the injectability of a brushite cement. Injectability tests were performed by placing the cement paste into a 10 mL syringe (2 mm diameter aperture; 13 mm diameter cartridge), and then mounting a compressive load (5 kg) on top of the plunger to start injection, until the paste was no longer injectable. The percentage of injectability was determined by the ratio between the mass of the paste that could be expelled from the syringe and the initial mass of the paste inside the syringe.

plate-like crystals in the reference and in the cements containing 20 mol% Si^{4+}, and additional sphere-like crystals in the cements containing 20 mol% Si^{4+}. A more rounded morphology was observed with increasing Si^{4+} content, while tube-like structures composed of rounded nanocrystals appeared for 60 and 80 mol% Si^{4+}.

1.2.3. Injectability

As aforementioned, several organic additives have already been investigated to improve the brushite cement injectability. However, injectability can also be affected by dopant ions. Saleh et al. [24] observed a strong improvement of the injectability of brushite cement by Mg^{2+} addition (Fig. 7 A). Up to 77% injectability was reported for a Mg^{2+} content of Mg/(Mg+Ca) = 0.1, compared to only 10 % injectability obtained for the reference. The enhanced injectability was related to an increased setting time.

A similar effect was observed for cements co-doped with Mn^{2+} and Sr^{2+} (Sr^{2+} concentration: 5 mol%; Mn^{2+} concentration: 0, 0.3 and 0.7 mol%) [25]. In this case, the injectability of the cements doped with 0.7 mol% Mn^{2+} was slightly lower than that with 0.3 mol% Mn^{2+} when an aqueous solution containing 15 wt% citric acid, 10 wt% poly(ethylene glycol) and 0.5 wt% hydroxyl propyl methylcellulose was used as a mixing liquid. Only a marginal increase of the injectability was observed for doping the cements with Sr^{2+} alone, by using mixing liquids containing sucrose or fructose. The reference was not injectable at all for all mixing liquids. Taha et al. [26] reported an increase of the injectability by Sr^{2+} doping, up to 66% for 6.6 wt% Sr^{2+} (Fig. 7 B), which was also related to an increase of the setting time. For higher concentrations, the injectability decreased again, in accordance with a decrease in setting time, related to monetite formation.

1.2.4. Mechanical properties

The mechanical properties of hardened bone cements are relevant, especially when it comes to load-bearing applications. Some approaches towards the improvement of the strength of brushite cements have been developed, such as fiber reinforcement [82], or utilizing the reinforcing effect of residual β-TCP particles [83]. Furthermore, it has to be considered that ionic dopants can have a positive or negative impact on the mechanical properties.

Alkhraisat et al. [23] observed a decrease of diametral tensile strength of Mg^{2+} containing brushite cement for lower Mg^{2+} contents up to 26.67 mol%, which according to the authors might have resulted from reduced microhardness of the brushite due to crystal defects. The strength recovered for higher Mg^{2+} contents, probably due to the formation of newberyite ($MgHPO_4{\cdot}3H_2O$), which led to a denser cement matrix. Saleh et al. [24] observed an increase of compressive strength (CS) with increasing Mg^{2+} content. A CS of only 1.32 MPa was obtained for the reference, while it strongly increased up to 20.98 MPa for a cement with a Mg^{2+} content of Mg/(Mg+Ca) = 0.1. This effect was explained by the reduced porosity of the Mg^{2+}-doped cements.

Cement containing β-TCP doped with 1 mol% Ag^{+} showed an increase of the CS by 30 % in the study reported by Ewald et al. [35]. In contrast, a reduction of CS by Ag^{+} addition was observed by Rau et al. [22]. CS was reduced to 4.0 ± 1.0 MPa (0.6 wt% Ag^{+}) and 1.5 ± 1.0 MPa (1 wt% Ag^{+}), while CS of 6.5 ± 1.0 MPa was obtained for the reference. The different behavior observed in those two studies might be explained by the formation of $CaAg(PO_3)_3$ [22], with no secondary phases detected [35].

Fe^{3+} was reported to have a positive impact on the CS of brushite cements [21]. The CS was more than doubled by doping β-TCP with 0.5 wt% Fe^{3+} after 1 day of hardening [21]. This was explained by the presence of small-sized brushite crystals, resulting in a reduction of porosity.

Co-doping with Mn^{2+} and Sr^{2+} was seen to be beneficial with respect to CS. The highest CS was obtained for β-TCP containing 5 mol% Sr^{2+} and 0.32 mol% Mn^{2+}. While the CS decreased for cements with 5 mol% Sr^{2+} and 0.7 mol% Mn^{2+}, it was still above the value obtained for the cements doped with 5 mol% Sr^{2+} only [25]. The improved CS was explained by the reduced porosity of the hardened cement. As no reference without Sr^{2+} was investigated with respect to CS in this study, the effect of Sr^{2+} alone was not determined. Still, Taha et al. [26] observed a remarkable increase of CS from 1.32 to 34 MPa for adding 6.6 wt% Sr^{2+} into β-TCP, while the CS decreased for higher concentrations.

In contrast, other ions were reported to have a negative impact on CS. Addition of 1.2 wt% Co^{2+} reduced the CS from 3.17 ± 1.04 MPa to 1.09 ± 0.21 MPa, being less pronounced for lower Co^{2+} concentrations [28]. Reduction of CS was further observed in cements containing β-TCP with 10 and 50 mmol of Co^{2+} [18]. Cu^{2+} and Cr^{3+} were reported to decrease the CS when added in concentrations of 50 mmol, while a concentration of 10 mmol had no noticeable effect [18].

Vahabzadeh et al. [29] observed a slight increase of CS on the cements containing 1.1 wt% Si^{4+}, from 4.78 ± 0.21 MPa to 5.53 ± 0.53 MPa, while lower Si^{4+} concentrations did not have any significant effect. In another study, the cementsĆS was reported not to be affected by the addition of 0.5 wt% Si^{4+}, while addition of 0.25 wt% Zn^{2+} resulted in a decrease of CS [32].

1.2.5. Ion release from brushite cements

In order to assess the biological impact of dopant ions into brushite cements, it is highly relevant to understand how they are released from the cement to the surrounding liquid, as they can only be effective there. In addition to the release performance of the dopant ion, its effect on the release of Ca^{2+} and phosphate ions can also be of biological relevance. The release profile of the corresponding ions can be dependent on the ion type, as well as on the cements composition.

In the cements investigated by Alkhraisat et al. [23], the sample containing 26.67 mol% Mg^{2+} showed an initial burst release of Ca^{2+} and Mg^{2+}, while a low constant release of both ions occurred for 66.67 mol% Mg^{2+}. Saleh et al. [24] observed a significant increase of the cation release after 7 days due to Mg^{2+} incorporation, especially for the highest Mg^{2+} concentration (Mg/(Mg+Ca) = 0.1). This was explained by a lower degree of crystallinity of the Mg^{2+}-doped cement.

Ewald et al. [35] reported a dependence of Ag^{+} release on the surrounding medium. The Ag^{+} release was low for PBS, whereas it was remarkably higher in lysogeny broth. The release level was more or less constant during 7 days, in the range of approximately 25–30 µg. Rau et al. [22] observed a release of 25 µg/L and 43 µg/L, respectively for 0.6 and 1.0 wt% Ag^{+} content in β-TCP, in TRIS-HCl buffer solution at 37°C. As a solid to liquid ratio of 0.5 g / 100 mL was applied for the insertion of crushed cement into the solution, this corresponded to a release of 5 µg/L and 8.6 µg/L respectively, for 0.6 and 1.0 wt% Ag^{+} content in β-TCP, from 1 g of cement. A plateau, indicative of equilibrium, was reached after 15 days. Thus, the ion release was below the concentrations expected to be toxic, i.e. 100 µg/L in the blood [84].

The release of Fe^{3+} from a brushite cement determined at 37 °C in TRIS-HCl buffer solution at pH=7.4 was 0.313 ± 0.003 mg/mL (15.7 mg Fe^{3+} released from 1 g of crushed cement with the applied solid to liquid ratio of 1 g / 100 mL) and therefore, one order of magnitude lower than the toxicity level [21].

Schamel et al. [18] detected an initial burst release of Cu^{2+} for samples containing either 10 or 50 mmol Cu^{2+}, followed by a lower constant release. This burst release was attributed to the possible presence of $CuHPO_4$, which has a high solubility comparable to brushite. Having a rhombohedral structure, this crystalline phase is not isostructural to the triclinic monetite ($CaHPO_4$) [85]. Furthermore, a reduction of phosphate release was observed by Cu^{2+} addition. A comparable observation was made for Co^{2+} in the same study, where the burst release was explained by the highly soluble $CoHPO_4$. In contrast to this, a continuously low release rate was observed for Cr^{3+}, which was explained by the low solubility of chromium phosphate. Furthermore, phosphate release was reduced in the samples containing 50 mmol Cr^{3+}.

For Zn^{2+}-doped cement, releases of 0.30 ± 0.01 and 0.10 ± 0.01 µg/L were observed for contents of 0.6 and 1.2 wt% Zn^{2+}, respectively, in TRIS-HCl buffer at pH=7.4 [30]. A solid to liquid ratio of 0.5 g / 100 mL yielded releases of 0.060 µg/L and 0.020 µg/L Zn^{2+}, respectively for 0.6 and 1.2 wt% Zn^{2+} and 1 g of brushite cement. The lower release obtained for higher dopant concentrations was attributed to the decrease of the dissolution rate of Zn-doped TCP. Torres et al. [25] reported a decrease of Sr^{2+} release in Sr^{2+} and Mn^{2+} co-doped β-TCP cements. Furthermore, they observed a preferential leaking of the Mn^{2+} ion. Generally, the Mn^{2+} release was higher for cements containing higher ion concentration.

Aparicio et al. [81] noticed a strong ions release effect of Si^{4+} doping. An initial burst release of 1155 and 990 ppm for Ca^{2+} and phosphate, respectively, followed by a continuous release, was observed for the undoped cements after 7 days of immersion in double-distilled water. In the cements 40 % Si-CPC and 80 % Si-CPC, a release of SiO_4^{4-} ions of 33 and 38 ppm was observed after 3 days of incubation. For Se-doped brushite, a higher release rate was observed for Se^{4+}, compared to Ca^{2+} and phosphate, which was explained by the possible adsorption of selenite ions on the surface of brushite crystals [80].

1.3. Biological performance of ion-doped brushite cements

1.3.1. Cell growth, viability and proliferation

The viability and proliferative behaviours are directly dependent on the nature and amount of dopant ions in the materials [36]. While some ions have the potential to promote cell viability, others can have toxic effects on cells if they are added in too high concentrations. In order to avoid these toxic effects, it is highly relevant to assess the concentration-dependent influence of each dopant ion on cell growth and viability.

A positive proliferative effect of Cu^{2+} on human glial E297, murine osteoblastic K7M2 and especially, human primary lung fibroblasts cells, can be found in the 1 – 2.5 mg/mL dose range (16 – 39 mM) [38]. Likewise, Schamel et al. [18] did not find any negative effects on hMSCs proliferation performed for Cu^{2+} concentrations $\leq$ 100 μM, while 250 μM resulted in a decrease of the cell number after day 7 and a concentration of 500 μM even led to cell death after 7 days (Fig. 8 A). For Co^{2+}, cell proliferation was not negatively affected up to a concentration $\leq$ 50 μM. 250 μM led to a significantly reduced cell proliferation, whereas 500 μM caused a continuous decrease of cell number. No negative impact on cell proliferation was observed for Cr^{3+} up to 250 µM, and only at 500 µM, the cell number was significantly reduced [18]. In direct cell culture, no cells were detected on Co50 and only small number of cells on Co10 (Fig. 8 B). For Cr^{3+}, a proliferation higher or similar to the reference was observed for 50 mmol concentration in indirect culture, while proliferation was diminished for 10 mmol Cr^{3+}. This was attributed to a decrease of Ca^{2+} level measured for 10 mmol Cr^{3+}. In direct culture, an enhanced cell proliferation compared to reference was observed for Cr^{3+} doped cement, especially for 50 mmol Cr^{3+}. Still, the authors explained that this effect might also result from the altered cement morphology observed for this sample.

In another study from Cummings et al. [77], no effects of MG-63 cell growth on brushite cements by different Co^{2+} concentrations up to 1 wt% doped into the β-TCP content was noticed. Ag^{+}-substituted brushite showed low toxicity when cultured with human adipose-derived stem cells (ADSCs) up to 10 mol% Ag [36].

In the case of doping brushite cements with Fe, a high cellular activity was observed for Fe concentration up to 0.50 wt%, while a higher concentration of ~1.00 wt% resulted in adverse effects on cell morphology and proliferation [21,40].

Multiple advantages on proliferation and osteogenic differentiation were also observed with Sr^{2+} and low concentration of Mn^{2+} [25,33]. For example, Sr^{2+} and Mn^{2+} co-doped brushite cements cultured on human MG63 osteoblastic cells have shown the best proliferation and differentiation results obtained for cements con-

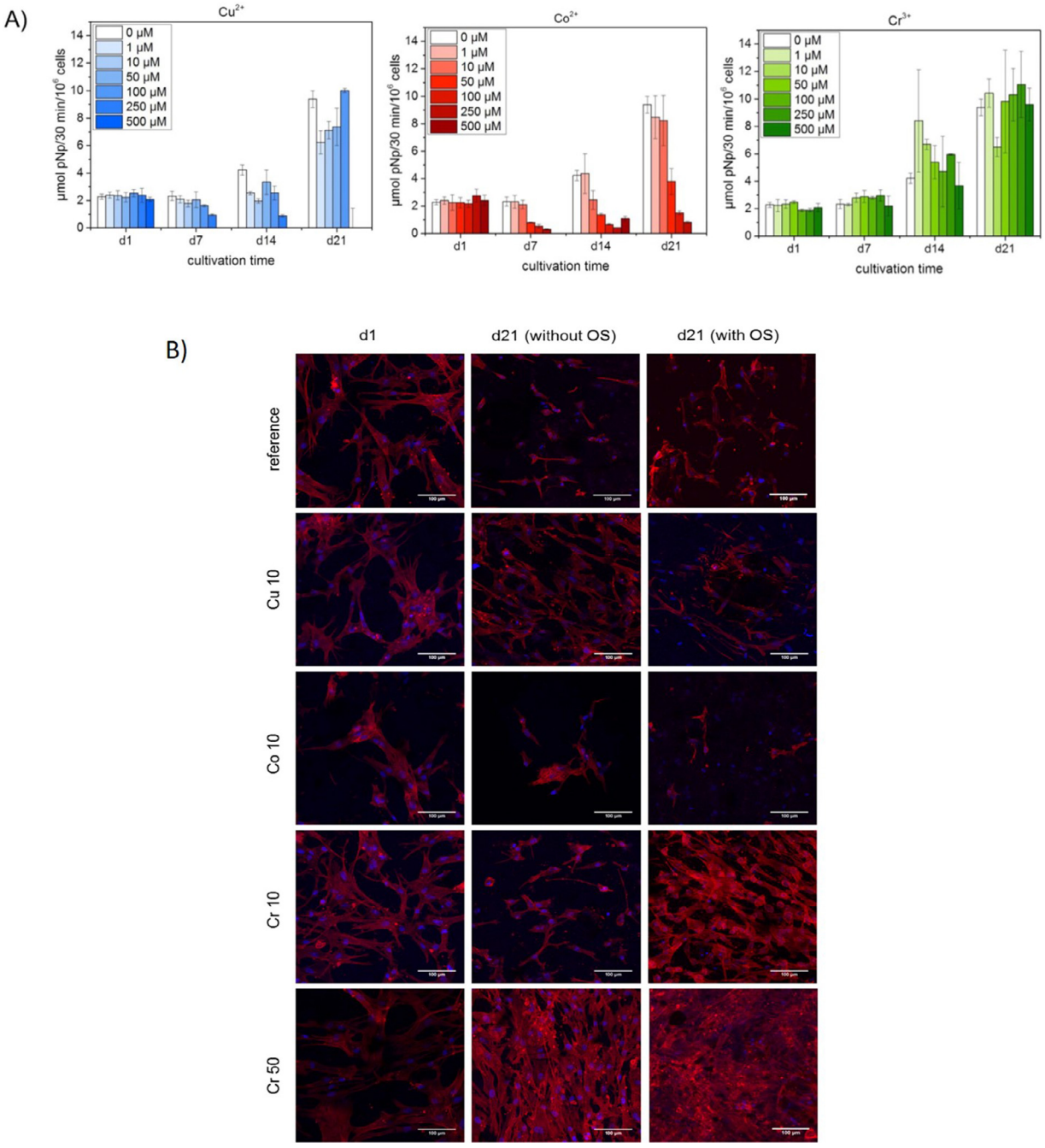

Fig. 8. Viability of hMSCs after 1 and 21 days of culture: A) in the presence of Cu^{2+} (A), Co^{2+} (B) and Cr^{3+} (C) added to the cell culture medium using different concentrations, and B) in the cement surfaces, with and without osteogenic supplements (OS). Reprinted with permission from [18].

taining 5 mol% Sr^{2+} only or 5 mol% Sr^{2+} and 0.32 mol% Mn^{2+} [25]. Accordingly, the highest cell density was observed on the surface of discs with 5 mol% Sr^{2+} and 0.32 mol% Mn^{2+}, showing better spreading and adherence of the cells to the substrate. It was further reported that the cell viability of MG63 pre-osteoblastic cells was increased by addition of Sr^{2+} for all Sr^{2+} concentrations investigated.

An enhancement of cell proliferation was detected for adding Si^{4+} in high concentrations. A more than threefold enhancement was reported for 80 mol% Si^{4+}, attributed to the ion release [81]. Furthermore, an enhancement of cellular adhesion induced by Si^{4+} was observed. In contrast, a higher cytotoxicity was observed for Se-doped brushite, compared to the reference, which corresponds to the release kinetics. The toxicity decreased with increase of dilution fold [80].

An interesting approach to obtain a ZrSi-doped brushite cement was reported by substituting the precursor β-TCP with baghdadite ($Ca_3ZrSi_2O_9$). This resulted in cements with enhanced proliferation activity of primary human osteoblast, with very low effect on the mechanical properties for up to 50 wt% substitution, and a strong reduction in phosphate release [86].

1.3.2. *Osteoclast activity* / in vivo *biodegradation*

Considering that brushite cements can be resorbed by physicochemical dissolution in the body, osteoclast activity can still play

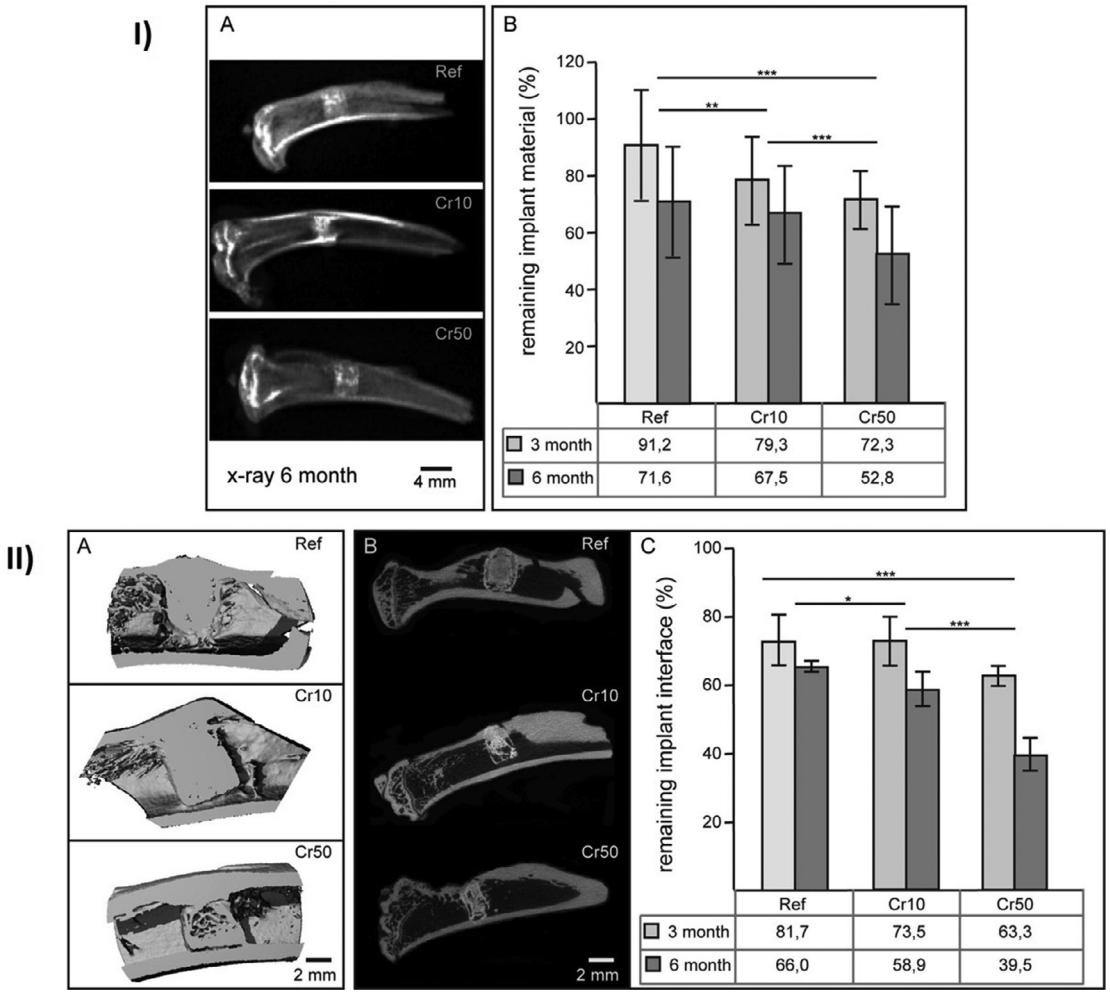

Fig. 9. Cr^{3+}-doped brushite cements explants: I) Radiographic analysis after 6 months of implantation in rat tibia (A) and material resorption after 3 and 6 months of implantation (B); $^{**}p<0.01$, $^{***}p<0.001$; II) Micro-CT analysis of the defect area after 6 months of implantation (A); Sagittal section plane (B), and Material resorption after 3 and 6 months of implantation (C); $^{*}p<0.05$, $^{***}p<0.001$ p-level. Cr 10: 10 mmol Cr^{3+}; Cr 50: 50 mmol Cr^{3+}. Reprinted with permission from [39].

an additional role in the biodegradation of these type of materials [10]. Furthermore, the presence of ionic dopants has shown important effects on the biodegradation and consequently on bone formation [36,40,43]. For example, Si^{4+} was reported to increase the activity of osteoclast like cells, while the amount of Si^{4+} doping did not affect the RAW 264.7 monocyte adhesion [29]. All Si^{4+} doped brushite cements showed higher tartrate resistant acid phosphatase (TRAP) activity compared with undoped brushite cements, which signified the enhancement of osteoclastogenesis by Si^{4+} doping. An amount of 0.5 wt% Si^{4+} addition appeared to be the optimum with respect to osteoclast-like-cell differentiation.

Another study by Rentsch et al. [39] showed an increase of osteoclast activity after 3 and 6 months of implanting brushite samples doped with 10 and 50 mmol Cr^{3+} in proximal tibia bone defects in rats, being more pronounced for higher Cr^{3+} concentration (Fig. 9). This also resulted in a higher resorption rate, supported by the higher resorbability of the Cr^{3+} doped material. They further observed a significant increase of the *in vivo* degradation of the materials by Cr^{3+} addition, with only 53% detected after 6 months of implantation (Fig. 9 I). Moreover, a decrease of Cr^{3+} content in the implanted material from 3 to 6 months was observed, with approximately 40% material remaining in the implantation site, after 6 months of implantation (Fig. 9 II). The release of Cr^{3+} resulted in positive effects on cement degradation, osteoclasts activity and new bone formation. The significant resorption of the cements can also be attributed to the use of phytic acid as setting retarder, which influences the cytocompatibility, and consequently bone cell activity and remodeling [87].

The release of ions incorporated in direct or indirect way into the cements, has also shown effectiveness to increase the biological performance of the materials. An example is the combination of brushite cements (BR) and bioglass 45S5, which contains Si^{4+}, Ca^{2+} and P^{3-} ions, that results in increased material resorption and bone tissue integration [88]. *In vitro* assays of the composite cements of brushite with 40% bioglass microspheres (BR/BM) seeded on MC3T3-E1 cells showed a positive effect of ionic release and dissolution products on cell growth and proliferation (Fig. 10 a and b). Large number of nuclei was observed in the materials after 14 and 21 days of culture with osteopontin (OPN) expression higher in the composite materials at 14 days (Fig. 10 c and d). Ca^{2+} and Si^{4+} ions released from the cements were able to produce a superficial layer that interacts with cells stimulating cell attachment, proliferation and differentiation indicating retention of solubility of the bioglass.

Osteoclasts fusion of peripheral blood mononuclear cells have also been shown to decrease with high Sr^{2+} release from brushite cements containing gelatin [89]. The osteoclast related gene expression markers DC-Stamp and CD44 were downregulated when in contact with the materials.

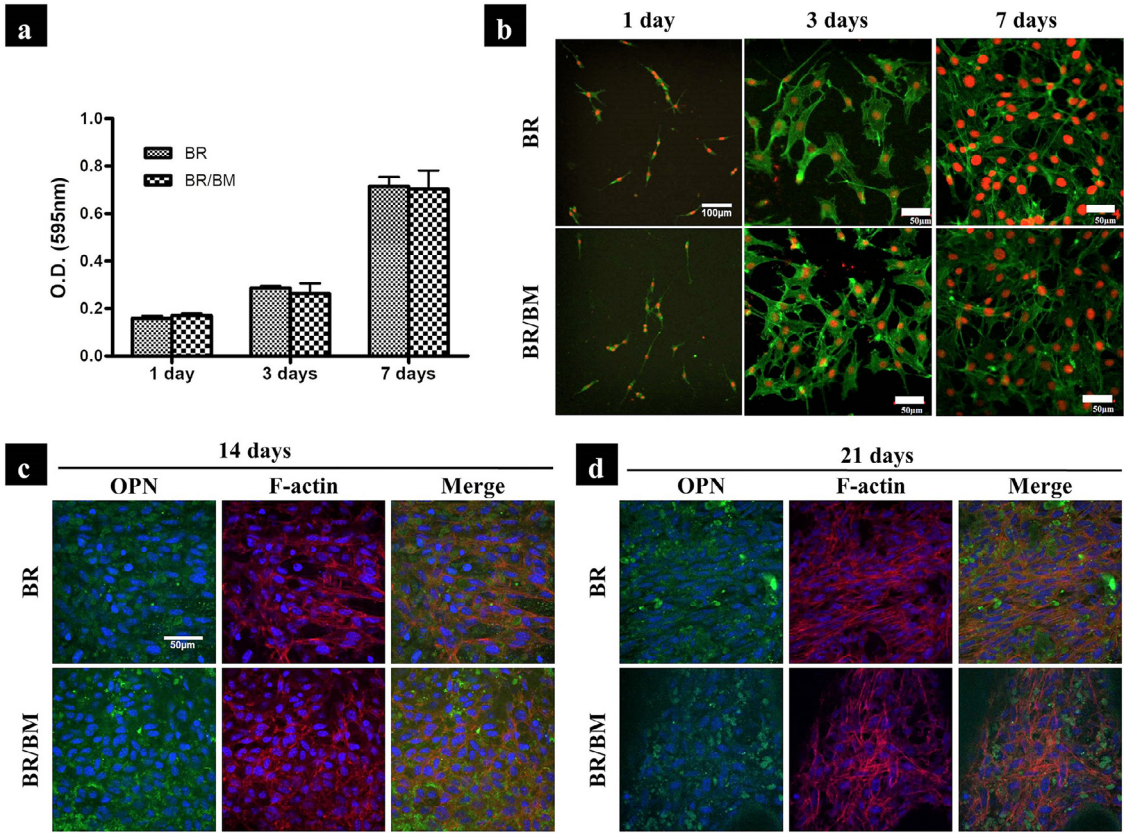

Fig. 10. *In vitro* biocompatibility tests using MC3T3E1 cells cultured on the cements: MTT assay (a); F-actin staining (b); Immunofluorescence detection micrographs of osteopontin (OPN) expression after 14 (c) and 21 (d) days in osteogenic conditions. Reprinted with permission from [88].

1.3.3. Osteogenesis and Angiogenesis

The mechanism involving bone formation is centred on osteogenesis, strongly linked with angiogenesis or blood vessel formation. Vascularisation is essential to engineer functional implants for bone repair and regeneration, when blood vessels are concerned for oxygen and nutrients delivery [90]. One of the main beneficial properties of CaPs-based materials is their osteoconductive capacity of new bone formation. Recently, CaPs ceramics are also recognized to possess intrinsic osteoinductivity due to their capacity to induce new bone formation in nonosseous sites in the absence of growth factors and signalling molecules [91]. This phenomenon is related to the materialsśtructural and physicochemical properties, such as the case of ion incorporation. Particular importance may be therefore given to ionic dopants involved in osteogenesis and angiogenesis induction to regulate the bone repair process [12]. For example, an osteoinductive effect of brushite cements, containing β-TCP doped with 0.49 wt% and 1.09 wt% Fe, was observed from high levels of osteocalcin and Runx2 in MC3T3-E1 cells [21]. However, the expression of Runx2 was higher in the cements with lower Fe content, indicating that the amount of Fe in the cements may be adjusted for bone induction/growth achievement.

The incorporation of Cu^{2+}, Co^{2+} or Cr^{3+} is also of interest. A study by Schamel et al. [18] showed human mesenchymal stromal cells attaching and dispersion in the cements with low amounts (10 mmol/mol β-TCP) of Cu^{2+}, Co^{2+} or Cr^{3+}, after 1 day of culture. For higher amounts (50 mmol/mol β-TCP), the cells were observed only on Cr^{3+}-doped cements and ALP activity increased with increasing Cr^{3+} amounts, indicating osteogenic differentiation. Furthermore, the highest rate of newly formed bone after 6 months of cements implantation in male adult Wistar rats was observed for 50 mmol Cr^{3+} (Fig. 11 I) [39]. Lamellar bone has grown from the defect margin into the central part, showing Haversian canals osteons (Fig. 11 II).

Si^{4+} and Zn^{2+} are other dopants known for their beneficiary effects on bone growth and angiogenesis [32,43]. The osteogenic potential of 0.25 wt% Zn+0.5 wt% Si-doped brushite cements was observed by well matured new tissue formation after 3 months of implantation in epiphyseal femurs of New Zealand white rabbits, owing to Zn/Si doping [43]. When the composites were cultured with endothelial cells, a favored survival was observed through tube formation and higher functionality in terms of nitric oxide secretion, proving the ability of Si/Zn dopants in triggering angiogenic signalling (Fig. 12). Similarly, an acceleration of neoosseous formation, despite high osteoclast activity, was also observed for higher (0.5, 0.8, and 1.1 wt%) Si^{4+}amounts [29]. *In vivo* studies were carried out by implanting these cements in rat distal femurs showing a complete bone formation after 12 weeks and blood vessel formation after 4 and 8 weeks. Significant enhancement of vasculogenesis was observed at 8 weeks of implantation due to the presence of Si^{4+} and its amount (Fig. 13).

A different approach to evaluate the role of ionic dopants on brushite cements were reported using β-TCP synthesized from eggshells as brushite precursor [92]. *In vivo* studies of the cements performed in rat calvarial bone defect for 12 weeks revealed faster degradation and accelerated bone formation. New blood vessels and formation of woven bone on the edges of the defect were observed after 6 months of cement implantation. This enhanced bone regenerative capacity was attributed to the use of natural sources as eggshells, which contain relevant trace elements (e.g. Mg^{2+}, Sr^{2+}, Si^{4+}, F^{-}, K^{+} and Na^{+}) along with calcium, resulting in improved physicochemical and biological properties of the materials.

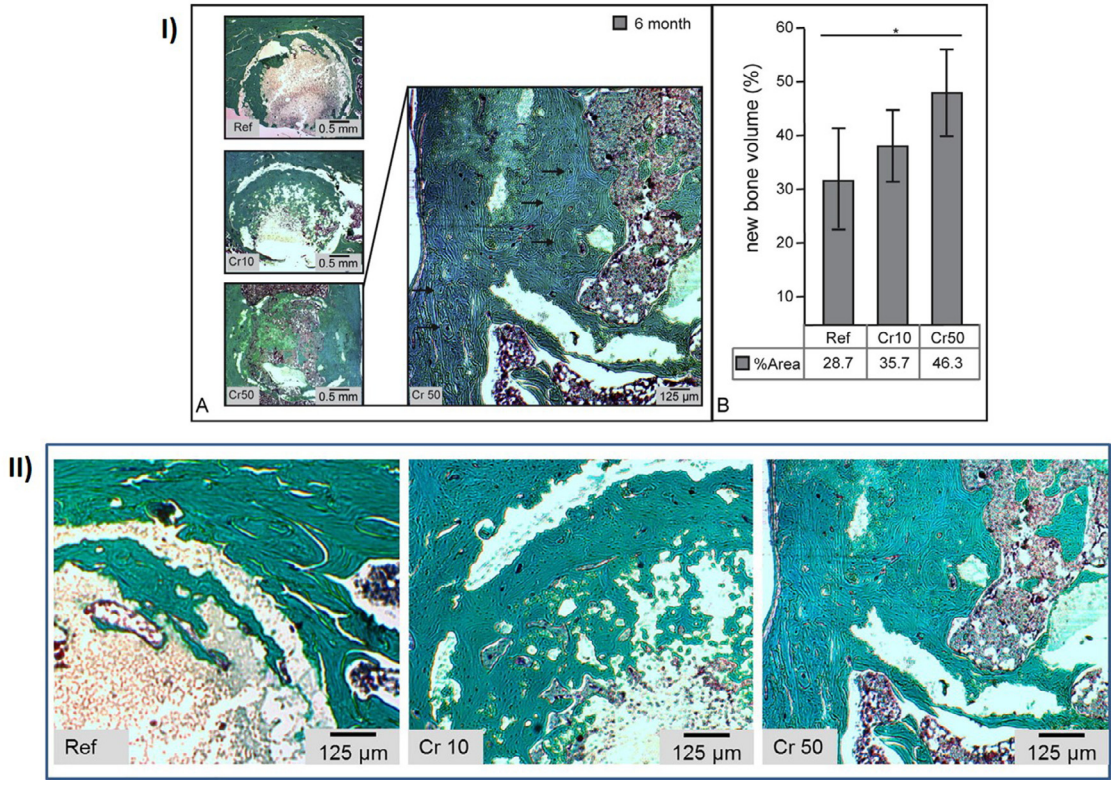

Fig. 11. Masson-Goldner trichrome staining of the explants of two animals per group after 6 months of implantation in male adult Wistar rats: I) Morphological (arrows = osteons including Haversian canals) (A) and Histomorphometric examination (n = 4; *p < 0.05) (B); II) Morphological evaluation of the histological sections. Reprinted with permission from [39].

$Sr^{2+}$is another relevant trace element known for its stimulatory effect on bone forming [12]. For example, Fang et al. investigated the *in vivo* performance of brushite cements doped with 5% Sr^{2+} by implanting them in alveolar bone defects in osteoporotic rabbits [37]. Results have shown the bone defect nearly filled after 8 weeks and highest β-FGF expression at 4 weeks of implantation.

1.3.4. Antibacterial activity

Complications as infection and inflammation of the defect site are serious issues in orthopaedics, leading to severe pain and in some cases, the implants removal. Hence, the use of antibiotics can be effective to contain these risks, but there is the problem of rising immunity of bacteria to traditional antibiotics [93]. Ionic dopants with antibacterial action appeared as a promising alternative approach to prevent infections in the medical field.

Ag^{+}, Zn^{2+} and Cu^{2+} are the most broadly used as ionic dopants with antibacterial properties [31,74,94-96]. Ag^{+} doped brushite cements were shown to reduce *Staphylococcus aureus* (*S. aureus*) adhesion with an antibacterial effect of 85 % and an inhibitory effect towards pathogenic *Escherichia coli* (*E. coli*) for Ag^{+} amounts of 0.6 and 1 wt%, while the effect was better for higher Ag concentrations [22,35].

The antibacterial effect of Cu^{2+} in brushite cements was also observed against Gram-negative bacteria *E. coli, Pseudomonas aeruginosa* (*P. aeruginosa*) and *Salmonella enteritidis* (*S. enteritidis*) for Cu^{2+} content of 0.3 wt% [38]. Interestingly, it was observed that the antibacterial activity of the cements was significantly higher than that of the CuTCP precursor powder, although the Cu^{2+} release from the powder exceeded that from the cement (Fig. 14). Since in the first hour the Cu^{2+} release from the cement was six times higher than that from the powder, it was concluded that this burst increases the antibiotic efficacy. Additionally, a synergy between cationic Cu^{2+} and a particular phase and aggregation state of the CaP carrier was proposed. Likewise, an inhibitory effect towards pathogenic *E. coli* was reported for cements containing 0.6 wt% Zn^{2+} [30]. It was observed that higher Zn^{2+} concentration led to the increase of the inhibition zone diameter.

Another interesting ion to be used against bacteria is Fe, particularly when possible side effects of Ag^{+}, like allergies or chronic skin changes, can occur [21,27,97]. Li et al. [27] reported the efficient antibacterial properties of Fe^{2+}-doped brushite cements against *S. aureus* and *P. aeruginosa*, but less efficiency against *E. coli* [27]. The authors attributed this fact to the interaction between the particles and cell surfaces or to the reaction of Fe^{2+} with endogenous hydrogen peroxide, which can induce lethality in bacteria. On the other side, Uskokovic et al. [21] observed that the antibacterial activity of Fe-doped brushite cements against *E. coli, S. enteritidis, P. aeruginosa*, and *S. aureus*, increased with Fe content increase (Fig. 15). Distinct inhibition zones were observed around all the cement compositions and an effect was interestingly noticed only against *E. coli* and *S. enteritidis* strains in broth assay with no critical effect of iron concentration.

1.3.5. Drug delivery systems

Osteomyelitis, a bone infection mainly caused by bacteria, mycobacteria or fungi, is a serious issue related with the treatment of bone defects. It is normally treated by operative debridement and antibiotic therapy [98]. Treatment of the disease can fail due to the inability to maintain high concentrations of antibiotics at the infection site. Filling the infected bone site with an antibiotic bone craft is a promising approach to ensure high local concentration of the antibiotic. CPCs have been investigated as good drug and bioactive signalling molecules (e.g. bone morphogenetic protein (BMP), recombinant human BMP-2 (rhBMP-2), insulin like growth factor (IGF), and transforming growth factor β (TGF-β)) carriers for mineralized tissues [99-106]. These materials have the advantage of a

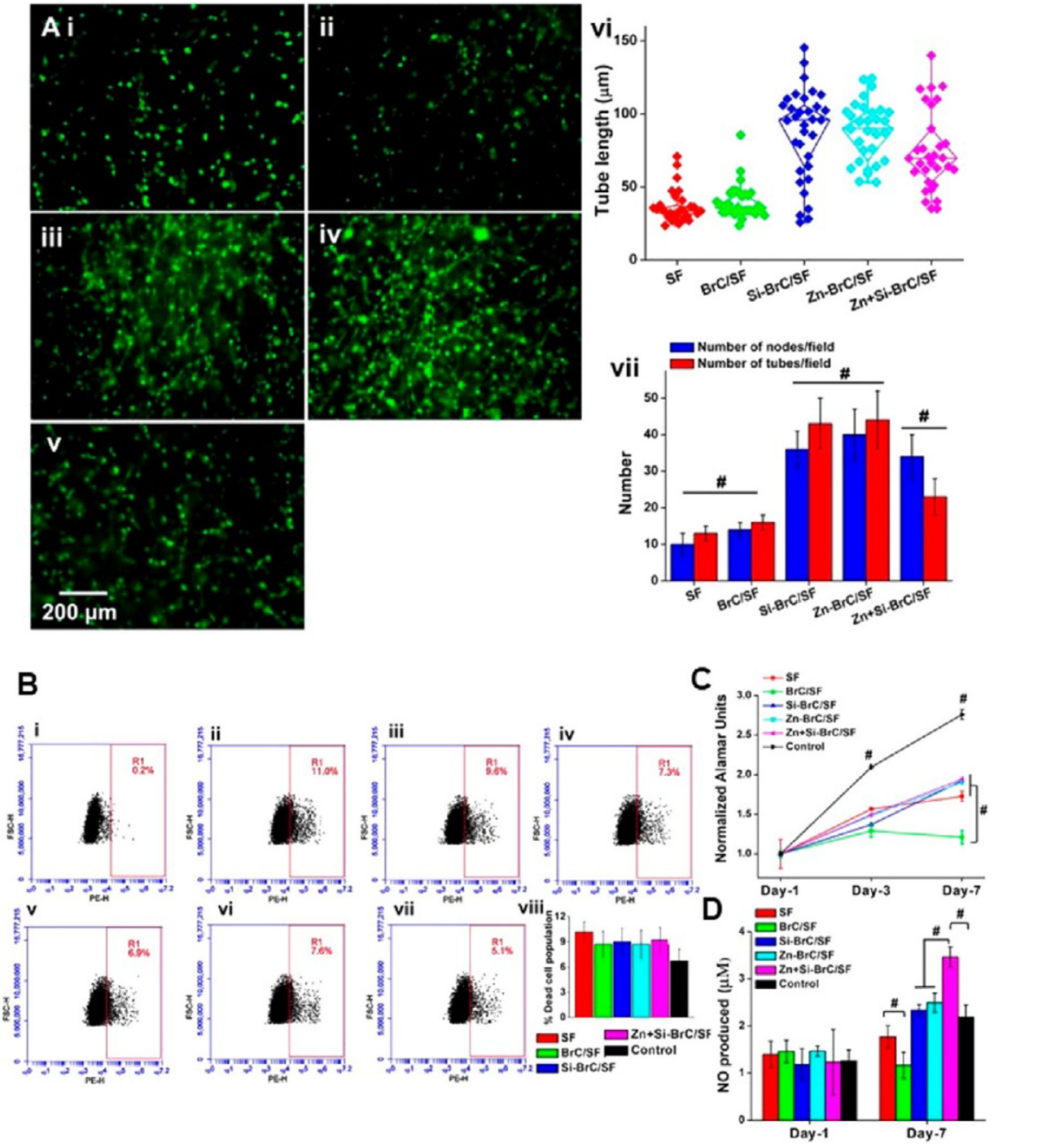

Fig. 12. Angiogenic performance of Si/Zn-doped brushite cements (BrC) /silk fibroin (SF) composites: (A) calcein-AM stained porcine endothelial cells for SF (i), BrC/SF (ii), Si-BrC/SF (iii), Zn-BrC/SF (iv), and Zn+Si-BrC/SF (v); (vi) tube length, and (vii) number of tubes and nodes noticed per imaging field from the fluorescent micrographs; (B) endothelial cells viability: unstained cells (i), SF (ii), BrC/SF (iii), Si-BrC/SF (iv), Zn-BrC/SF (v), Zn+Si-BrC/SF (vi), endothelial cells control (vii) and percentage of dead cell population (viii); (C) alamar blue assay; and (D) biochemical estimation of endothelial nitric oxide (NO) (#$p \leq 0.05$). Reprinted with permission from [43]. Copyright (2019) American Chemical Society.

low setting temperature, which also enables the incorporation of heat-labile drugs. The drug release profile is also relevant concerning to achieve the desired clinical outcome. One option to adjust the release profile is via the cement porosity, which can in turn be adjusted by liquid/cement ratio [107].

Another important issue is the incorporation of the drug inside CPC. The drug can be incorporated in the powder or in the liquid of the cements, and its release will depend on the cements degradation (Fig. 16): (i) the release is controlled by diffusion through the fluid permeating the cement, if its degradation is slower than diffusion (Fig. 16 a); (ii) the release is controlled by cement degradation, if it is faster than diffusion (Fig. 16 b); and (iii) in the cases of an apatite layer is formed, the drug diffusion can be delayed (Fig. 16 c) [101].

Although very few studies regarding ion-doped brushite cements used as drug and biomolecules carriers are reported, these biomaterials are very interesting for such purpose, due to their low setting reaction and intrinsic porosity [24,26,32,41]. For example,

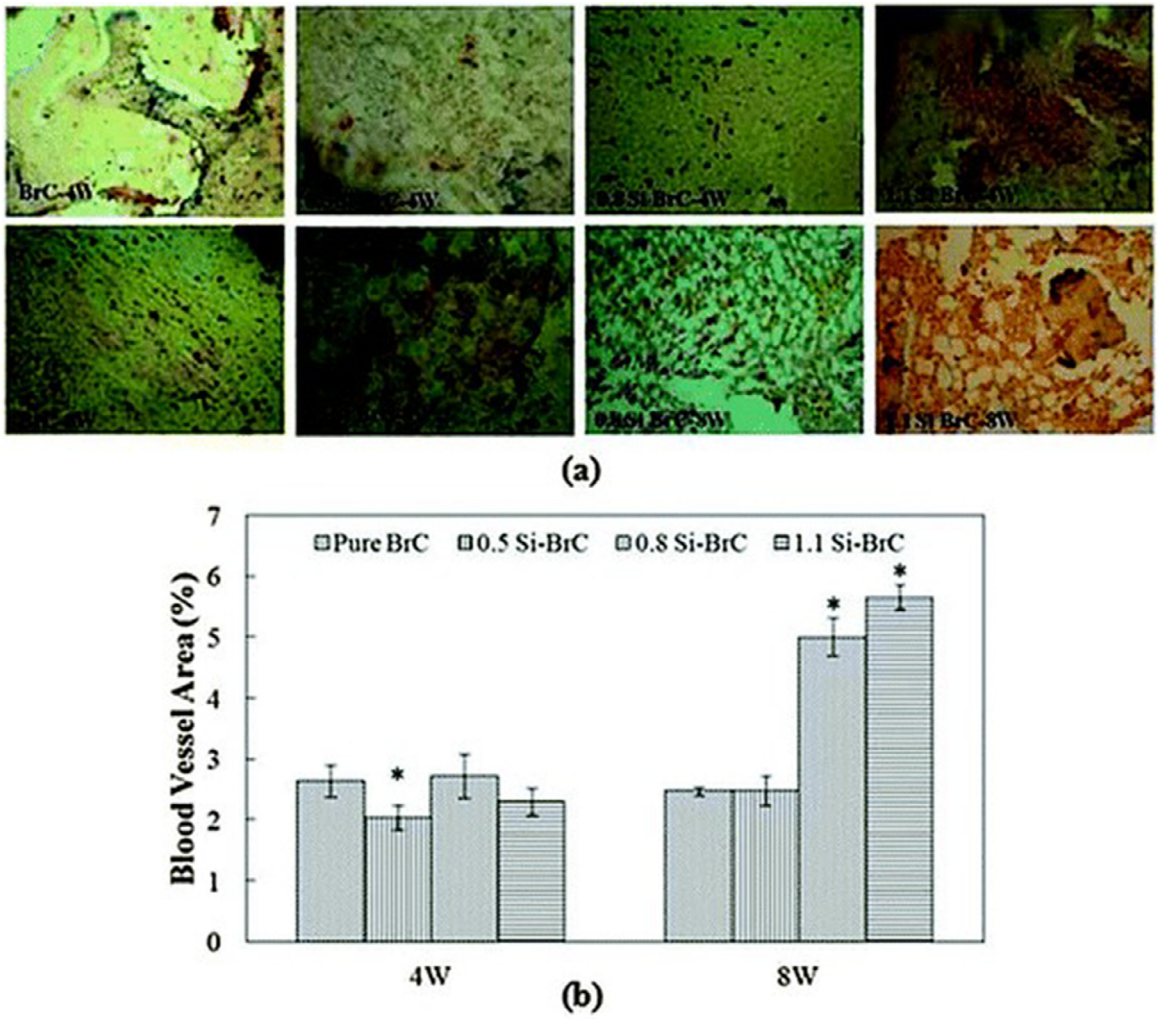

Fig. 13. (a) Photomicrographs of von Willebrand factor staining of the tissue sections after 4 and 8 weeks of implantation; and (b) histomorphometric analysis showing new blood vessel area. BrC: brushite cements. Si-BrC: Si doped BrC. Reprinted with permission from [29].

Cabrejos-Azama et al. [41] investigated a Mg^{2+}-doped brushite cement as a carrier for vancomycin delivery against *S. aureus* and most of Gram-positive bacteria. It was observed that the drug release was dependent of the amount of Mg^{2+} in the cements, being fast for 26.67 mol% MgTCP and slow for higher Mg^{2+} concentrations. In contrast, nearly no effect was observed when the drug was loaded by adsorption. Accordingly, the sample with 26.67 mol% Mg^{2+} showed an initial abrupt of vancomycin release, possibly owed to higher porosity and specific surface area of the cement. Saleh et al. [24] examined the release of gentamicin sulfate, amoxicillin and ampicillin trihydrate from brushite cements containing Mg^{2+}. They observed a burst release in the first 12 hours, which was attributed to a release of the drug adsorbed on the outer sample surface. This was followed by a controlled continuous release, which was explained by the release of the drug incorporated within the cement network. The release profiles showed a continuous drug release over 14 days, with cumulative releases of 99.3%, 87%, and 79%, respectively for gentamicin sulfate, amoxicillin, and ampicillin trihydrate.

In another study by Taha et al. [26], the use of brushite cements containing 6.6 wt% Sr^{2+} as a carrier for gentamicin sulfate, amoxicillin and ampicillin trihydrate was also investigated. It was observed an initial followed by a slow burst release for 14 days, with a cumulative release of 65%, 57% and 47% for undoped cements, respectively for gentamicin sulfate, amoxicillin, and ampicillin trihydrate (Fig. 17 a). A noticed increase of drug release was observed in the first 72 hours by using Sr-doped cements, of 96%, 87% and 73%, respectively for gentamicin sulfate, amoxicillin, and ampicillin trihydrate (Fig. 17 b).

Recently, the influence of Si doping (40% and 80% [Si/(Si+P)] molar ratio) for drug loading and delivery was evaluated in two different materials with different porosity and specific surface area, namely Si-doped β-TCP ceramics and Si-doped brushite cements [42]. It was observed that 98 % of vancomycin was released from the Si-ceramics after 168 hours, being slower than in undoped ceramics. This fact was attributed to an anomalous transport mechanism, according to the Korsmeyer-Peppas model. The release of 10 mg/mL vancomycin for Si-cements containing β-TCP with a [Si/(Si+P)] molar ratio of 40% and 80% was respectively, 93% and 62% after 157 hours. Therefore, the authors concluded that the vancomycin release rate was better controlled when Si was incorporated into the materials, and the cements with higher Si content presented a decreased and controlled release rate.

Ion-doped brushite cements have also been useful as growth factors delivery systems [32]. A study by Vahabzadeh et al. [32] reported that IGF-1 loading on 0.5 wt% Si/0.25 wt% Zn-doped cements presented reasonably enhanced new osseous tissue formation after 4 months of implantation in rabbit distal femurs, in comparison to unloaded cements. Furthermore, IGF-1 led to the formation of collagen network and bone cell colonization matrix.

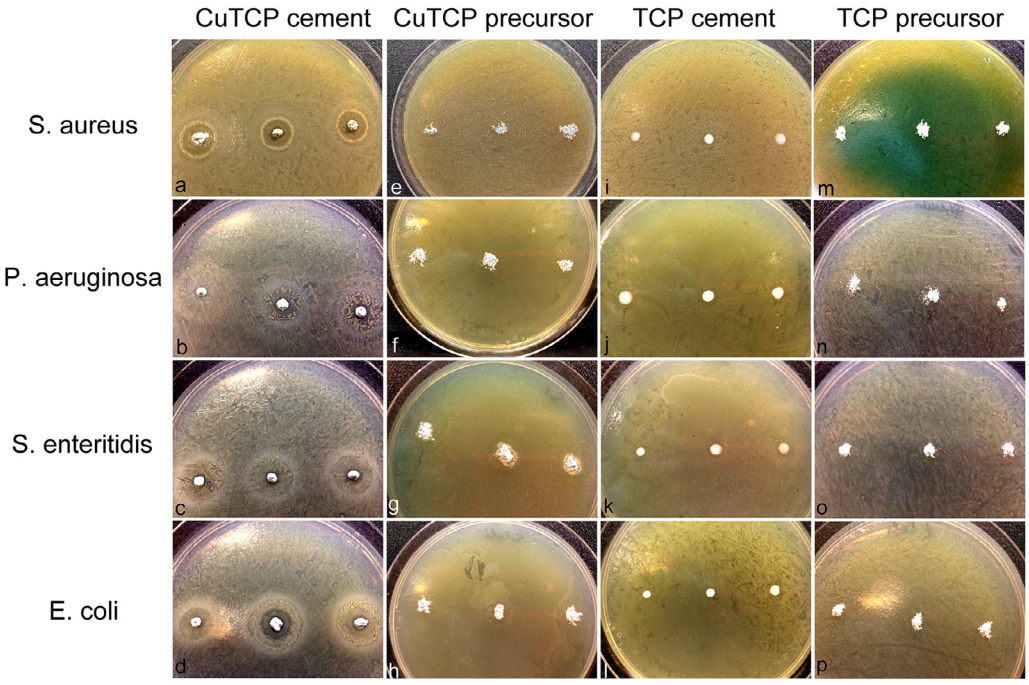

Fig. 14. Assays carried out against Gram-positive *S. aureus* (a, e, i, m) and Gram-negative *P. aeruginosa* (b, f, j, n), *S. enteritidis* (c, g, k, o) and *E. coli* (d, h, l, p). Bacterial inhibition zones around the CuTCP cement (a–d) and absent around the CuTCP precursor (e–h) and around TCP cement (i–l) and in TCP precursor (m–p). Reprinted with permission from [38].

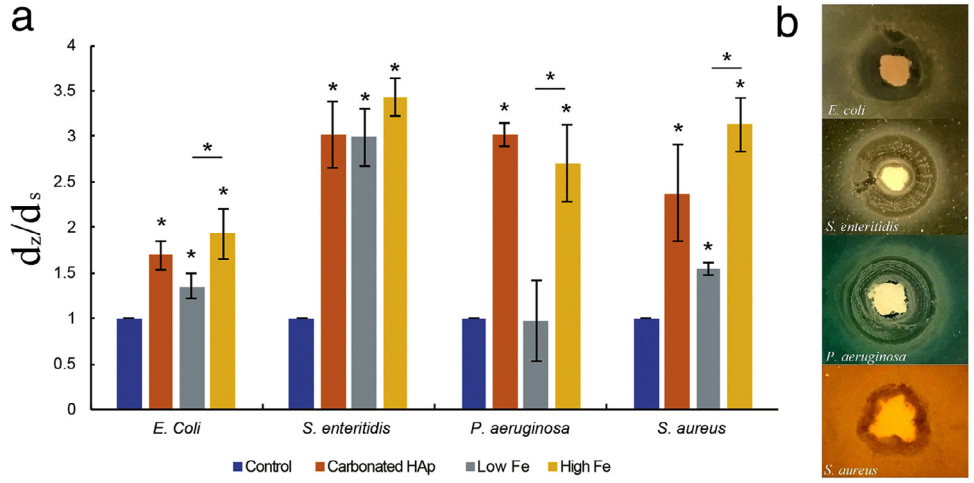

Fig. 15. Antibacterial assays of Fe-doped cements: I) diameter of the inhibition zone (dz) and diameter of the spherical cement sample deposit (ds) on an agar plate after 24 h inoculation with *E. coli, S. enteritidis, P. aeruginosa* or *S. aureus;* and II) visual images of bacteria inhibition zones around Fe-cements for different bacterial cultures. Carbonated HAp: with a precursor HAp component of the cement formulation; Low Fe: Fe-doped cement containing 0.49 wt%; High Fe: Fe-doped cement containing 1.09 wt%. Data are shown as averages with error bars representing standard deviation (*p < 0.05). Reprinted with permission from [21].

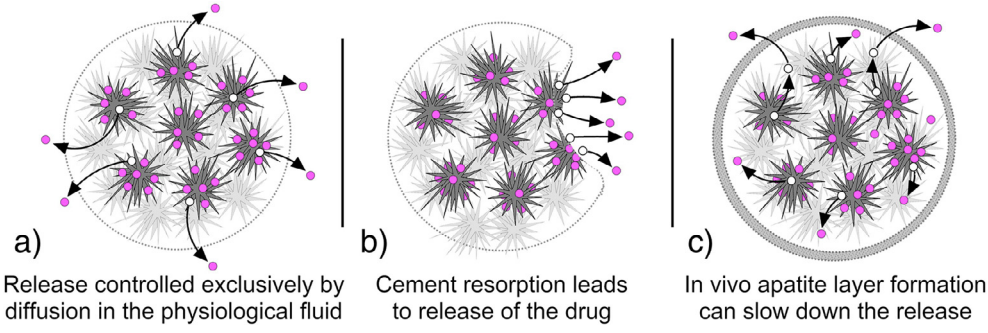

Fig. 16. Different states of drug release from CPCs. Adapted with permission from [101].

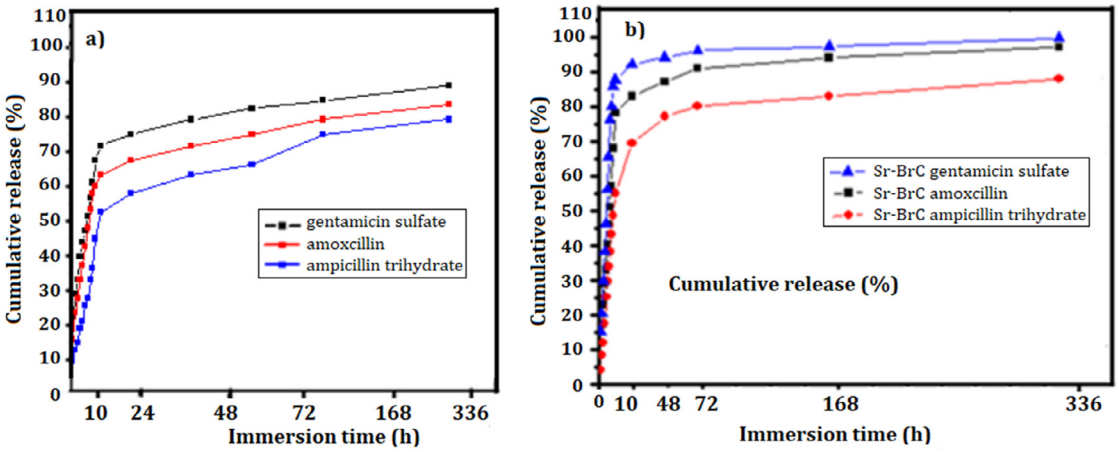

Fig. 17. Release profiles of gentamicin sulfate, amoxicillin, and ampicillin trihydrate evaluated in a) undoped brushite cements (BrC) and b) Sr-doped brushite cements (Sr-BrC). Reprinted with permission from [26].

2. Conclusions and future trends

Several properties of brushite cements can be effectively improved by the addition of inorganic dopants for the development of the next generation biomaterials for bone and periodontal defects repair and regeneration. Ionic substitutions or dopants can have an impact on various features, ranging from the biological performance like cell interactions, osteogenic/angiogenic potential or even antibacterial traits to physicochemical properties like setting time, injectability or mechanical performance. Sometimes synergistic effects can be reached, when ions with positive impact on the biological performance can also improve the setting performance or mechanical properties. But on the other hand, ion doping benefits with respect to one aspect can have a detrimental effect on other properties. Hence, for successful biomedical applications of ion doping, it is of high importance to assess the impact of each ion in all fields of relevant brushite cement properties. The concentration of the ion of interest needs to be carefully chosen in order to obtain sufficient efficacy with respect to the targeted properties, but at the same time to avoid negative side effects resulting from overdosage. The degradation of the cements, as well as the release profile for the specific ion need to be considered. Main concerns are related to adequate amounts of released ions in *in vivo* scenario, with positive therapeutic and regenerative levels.

Concerning the extensive research reporting the efficacy of CPCs as carrier materials for controlled drug/antibiotics/growth factors delivery to bone, further research needs to be devoted to ion-doped brushite cements. These cements possess fast resorption rate *in vivo*, which enhance the drug mobility for several therapeutic applications. Ion incorporation offers a high potential to provide bone regeneration capacity (e.g. Sr^{2+}, Zn^{2+}, Mg^{2+}, and Si^{4+}) and antibacterial activity (e.g. Ag^{+} and Cu^{2+}).

Despite the work performed so far, some obstacles remain that hinder a fast-clinical translation. Moreover, it has to be considered that data sets for ion-doped cements obtained from different studies are not directly comparable, since especially physical properties like setting time, injectability and mechanical properties are not only affected by dopant ions, but also by other factors like synthesis conditions and the resulting grain size of the starting powders, the LPR of the cement pastes and other possible cement additives as organic compounds. Therefore, in order to directly compare the effect of different ions on specific cement properties like the setting time, broader studies including the most promising ions would be highly valuable. Here, equal synthesis conditions, as well as cement paste compositions for all ions under investigation should be ensured to exclude the effect of other parameters. With respect to the biological performance, long-term studies and a deeper understanding of these dopants mechanism behaviour are still needed, for new biomedical products regulation and to turn them clinically accessible. Promising research directions that are being explored comprise 3D printing technology for the fabrication of personalized brushite-based scaffolds as bone grafts, able to promote bone ingrowth and osteoinductivity capability.

Statement of significance

Ion-doped brushite cements have unbolted a new era in orthopaedics with high clinical interest to restore bone defects and facilitate the healing process, owing its outstanding bioresorbability and osteoconductive/osteoinductive features. Ion incorporation expands their application by increasing the osteogenic and neovascularization potential of the materials, as well as their mechanical performance. Recent accomplishments of brushite cements incorporating bioactive ions are overviewed. Focus was placed on the role of ions on the physicochemical and biological properties of the biomaterials, namely their structure, setting time, injectability and handling, mechanical behaviour, ion release and *in vivo* osteogenesis, angiogenesis and vascularization. Antibacterial activity of the cements and their potential use for delivery of drugs are also highlighted herein.

Declaration of Competing Interest

None.

Acknowledgments

This study was funded by the Portuguese Foundation for Science and Technology (FCT) and the German Academic Exchange Service (Deutscher Akademischer Austauschdienst, DAAD) for the transnational cooperation FCT/DAAD 2018-2019. The authors also thank the funds provided under the distinctions attributed to JMO (IF/01285/2015) and SP (CEECIND/03673/2017). Furthermore, funding by the German Research Foundation (Deutsche Forschungsgemeinschaft, DFG), Grant Nr. HU 2498/1-1; GB 1/22-1, and the Emerging Talents Initiative of the FAU is acknowledged.

References

[1] M Bohner, U Gbureck, JE. Barralet, Technological issues for the development of more efficient calcium phosphate bone cements: A critical assessment, Biomaterials 26 (2005) 6423–6429.

[2] AR Amini, CT Laurencin, SP. Nukavarapu, Bone Tissue Engineering: Recent Advances and Challenges, Critical reviews in biomedical engineering 40 (2012) 363–408.
[3] W Wang, KWK. Yeung, Bone grafts and biomaterials substitutes for bone defect repair: A review, Bioact Mater 2 (2017) 224–247.
[4] W. Brown, A new calcium phosphate setting cement, J Dent Res 63 (1983) 672.
[5] SV. Dorozhkin, Self-setting calcium orthophosphate formulations: cements, concretes, pastes and putties, Int J Mater Chem 1 (2011) 1–48.
[6] M. Bohner, Calcium orthophosphates in medicine: from ceramics to calcium phosphate cements, Injury 31 (2000) D37-D47.
[7] U. Gbureck, Injizierbare Calciumphosphat-Zemente als Knochenersatzwerkstoff in niedrig belasteten Bereichen des Skelettsystems, Abteilung für Funktionswerkstoffe der Medizin und der Zahnheilkunde der Universität Würzburg, 2004.
[8] JC. Elliott, Structure and chemistry of the apatites and other calcium orthophosphates, Elsevier, 1994.
[9] AA Mirtchi, J Lemaitre, N. Terao, Calcium phosphate cements: study of the β-tricalcium phosphate—monocalcium phosphate system, Biomaterials 10 (1989) 475–480.
[10] Z Sheikh, YL Zhang, L Grover, GE Merle, F Tamimi, J. Barralet, In vitro degradation and in vivo resorption of dicalcium phosphate cement based grafts, Acta Biomaterialia 26 (2015) 338–346.
[11] S Bose, G Fielding, S Tarafder, A. Bandyopadhyay, Trace element doping in calcium phosphate ceramics to Understand osteogenesis and angiogenesis, Trends in biotechnology (2013) 31.
[12] S Bose, G Fielding, S Tarafder, A. Bandyopadhyay, Understanding of dopant-induced osteogenesis and angiogenesis in calcium phosphate ceramics, Trends in biotechnology 31 (2013) 594–605.
[13] RK. Rude, Magnesium deficiency: a cause of heterogenous disease in humans, Journal of Bone and Mineral Research 13 (1998) 749–758.
[14] SM Al-Ghamdi, EC Cameron, RA. Sutton, Magnesium deficiency: pathophysiologic and clinical overview, American Journal of Kidney Diseases 24 (1994) 737–752.
[15] PJ Marie, M Hott, D Modrowski, C De Pollak, J Guillemain, P Deloffre, et al., An uncoupling agent containing strontium prevents bone loss by depressing bone resorption and maintaining bone formation in estrogen-deficient rats, Journal of Bone and Mineral Research 8 (1993) 607–615.
[16] JY Reginster, E Seeman, MC De Vernejoul, S Adami, J Compston, C Phenekos, et al., Strontium Ranelate Reduces the Risk of Nonvertebral Fractures in Postmenopausal Women with Osteoporosis: Treatment of Peripheral Osteoporosis (TROPOS) Study, The Journal of Clinical Endocrinology & Metabolism 90 (2005) 2816–2822.
[17] MA Saghiri, A Asatourian, J Orangi, CM Sorenson, N. Sheibani, Functional role of inorganic trace elements in angiogenesis—Part II: Cr, Si, Zn, Cu, and S, Critical Reviews in Oncology/Hematology 96 (2015) 143–155.
[18] M Schamel, A Bernhardt, M Quade, C Würkner, U Gbureck, C Moseke, M Gelinsky, A. Lode, Cu2+, Co2+ and Cr3+ doping of a calcium phosphate cement influences materials properties and response of human mesenchymal stromal cells. Materials science & engineering C, Materials for biological applications 73 (2017) 99–110.
[19] A Bernhardt, M Schamel, U Gbureck, M. Gelinsky, Osteoclastic differentiation and resorption is modulated by bioactive metal ions Co2+, Cu2+ and Cr3+ incorporated into calcium phosphate bone cements, PloS one 12 (2017) e0182109.
[20] T Mokabber, HT Cao, N Norouzi, P van Rijn, YT. Pei, Antimicrobial Electrodeposited Silver-Containing Calcium Phosphate Coatings, ACS Appl Mater Interfaces 12 (2020) 5531–5541.
[21] V Uskoković, V Graziani, VM Wu, IV Fadeeva, AS Fomin, IA Presniakov, M Fosca, M Ortenzi, R Caminiti, JV. Rau, Gold is for the mistress, silver for the maid: Enhanced mechanical properties, osteoinduction and antibacterial activity due to iron doping of tricalcium phosphate bone cements. Materials science & engineering C, Materials for biological applications 94 (2019) 798–810.
[22] JV Rau, M Fosca, V Graziani, AA Egorov, YV Zobkov, AY Fedotov, M Ortenzi, R Caminiti, AE Baranchikov, VS. Komlev, Silver-Doped Calcium Phosphate Bone Cements with Antibacterial Properties, Journal of functional biomaterials 7 (2) (2016) 10.
[23] MH Alkhraisat, J Cabrejos-Azama, CR Rodríguez, LB Jerez, EL. Cabarcos, Magnesium substitution in brushite cements, Materials science & engineering C, Materials for biological applications 33 (2013) 475–481.
[24] AT Saleh, LS Ling, R. Hussain, Injectable magnesium- doped brushite cement for controlled drug release application, Journal of Materials Science 51 (2016) 7427–7439.
[25] PMC Torres, A Marote, AR Cerqueira, AJ Calado, JCC Abrantes, S Olhero, OAB da Cruz e Silva, SI Vieira, JMF. Ferreira, Injectable MnSr-doped brushite bone cements with improved biological performance, Journal of Materials Chemistry B 5 (2017) 2775–2787.
[26] A Taha, M Akram, Z Jawad, AZ Alshemary, R. Hussain, Strontium doped injectable bone cement for potential drug delivery applications. Materials science & engineering C, Materials for biological applications 80 (2017) 93–101.
[27] G Li, N Zhang, S Zhao, K Zhang, X Li, A Jing, X Liuc, T. Zhanga, Fe-doped brushite bone cements with antibacterial property, Materials Letters 215 (2018) 27–30.
[28] S Vahabzadeh, S Fleck, MK Duvvuru, H. Cummings, Effects of Cobalt on Physical and Mechanical Properties and In Vitro Degradation Behavior of Brushite Cement, JOM (2019) 315–320.
[29] S Vahabzadeh, M Roy, S. Bose, Effects of Silicon on Osteoclast Cell Mediated Degradation, In Vivo Osteogenesis and Vasculogenesis of Brushite Cement, Journal of Materials Chemistry B 3 (2015) 8973–8982.
[30] V Graziani, M Fosca, AA Egorov, YV Zobkov, AY Fedotov, AE Baranchikov, M Ortenzi, R Caminiti, VS Komlev, JV. Rau, Zinc-releasing calcium phosphate cements for bone substitute materials, Ceramics International 42 (2016) 17310–17316.
[31] X Li, G Li, K Zhang, Z Pei, S Zhao, J. Li, Cu-loaded Brushite bone cements with good antibacterial activity and operability, Journal of biomedical materials research Part B, Applied biomaterials (2020) 1–13.
[32] S Vahabzadeh, A Bandyopadhyay, S Bose, R Mandal, SK. Nandi, IGF-loaded silicon and zinc doped brushite cement: physico-mechanical characterization and in vivo osteogenesis evaluation, Integrative biology: quantitative biosciences from nano to macro 7 (2015) 1561–1573.
[33] T Wu, H Shi, Y Liang, T Lu, Z Lin, J. Ye, Improving osteogenesis of calcium phosphate bone cement by incorporating with manganese doped β-tricalcium phosphate, Materials Science and Engineering: C 109 (2020) 110481.
[34] K Paul, BY Lee, C Abueva, B Kim, HJ Choi, SH Bae, BT. Lee, In vivo evaluation of injectable calcium phosphate cement composed of Zn- and Si-incorporated β-tricalcium phosphate and monocalcium phosphate monohydrate for a critical sized defect of the rabbit femoral condyle, Journal of biomedical materials research Part B, Applied biomaterials 105 (2017) 260–271.
[35] A Ewald, D Hösel, S Patel, LM Grover, JE Barralet, U. Gbureck, Silver-doped calcium phosphate cements with antimicrobial activity, Acta Biomaterialia 7 (2011) 4064–4070.
[36] M Sayahi, J Santos, H El-Feki, C Charvillat, F Bosc, I Karacan, B Milthorpec, C Drouet, Brushite (Ca,M)HPO4, 2H2O doping with bioactive ions (M = Mg2+, Sr2+, Zn2+, Cu2+, and Ag+): a new path to functional biomaterials? Materials Today Chemistry 16 (2020) 100230.
[37] J Fang, W Dong, H Peng, Y Xu, W Jia, L Liang, Y. Liang, Study on reconstruction of rabbit alveolar bone defect with strontium-containing brushite bone cements, The Journal of Practical Medicine 34 (5) (2018) 720–724.
[38] JV Rau, VM Wu, V Graziani, IV Fadeeva, AS Fomin, M Fosca, V. Uskoković, The Bone Building Blues: Self-hardening copper-doped calcium phosphate cement and its in vitro assessment against mammalian cells and bacteria, Materials science & engineering C, Materials for biological applications 79 (2017) 270–279.
[39] B Rentsch, A Bernhardt, A Henß, S Ray, C Rentsch, M Schamel, U Gbureck, M Gelinsky, S Rammelt, A. Lode, Trivalent chromium incorporated in a crystalline calcium phosphate matrix accelerates materials degradation and bone formation in vivo, Acta Biomaterialia 69 (2018) 332–341.
[40] S Vahabzadeh, S Fleck, J Marble, F Tabatabaei, L. Tayebi, Role of iron on physical and mechanical properties of brushite cements, and interaction with human dental pulp stem cells, Ceramics International 46 (2020) 11905–11912.
[41] J Cabrejos-Azama, MH Alkhraisat, C Rueda, J Torres, C Pintado, L Blanco, López-Cabarcos E. Magnesium substitution in brushite cements: Efficacy of a new biomaterial loaded with vancomycin for the treatment of Staphylococcus aureus infections. Materials science & engineering C, Materials for biological applications 61 (2016) 72–78.
[42] J Lucas-Aparicio, Á Manchón, C Rueda, C Pintado, J Torres, MH Alkhraisat, López-Cabarcos E. Silicon-calcium phosphate ceramics and silicon-calcium phosphate cements: Substrates to customize the release of antibiotics according to the idiosyncrasies of the patient, Materials Science and Engineering: C 106 (2020) 110173.
[43] JC Moses, M Dey, KB Devi, M Roy, SK Nandi, BB. Mandal, Synergistic Effects of Silicon/Zinc Doped Brushite and Silk Scaffolding in Augmenting the Osteogenic and Angiogenic Potential of Composite Biomimetic Bone Grafts, ACS Biomaterials Science & Engineering 5 (2019) 1462–1475.
[44] A Laskus, J. Kolmas, Ionic Substitutions in Non-Apatitic Calcium Phosphates, Int J Mol Sci 18 (2017) 2542.
[45] AA Mirtchi, J Lemaître, E. Munting, Calcium phosphate cements: effect of fluorides on the setting and hardening of β-tricalcium phosphate-dicalcium phosphate-calcite cements, Biomaterials 12 (1991) 505–510.
[46] M Bohner, P Van Landuyt, H Merkle, J. Lemaitre, Composition effects on the pH of a hydraulic calcium phosphate cement, Journal of Materials Science: Materials in Medicine 8 (1997) 675–681.
[47] M Bohner, U. Gbureck, Thermal reactions of brushite cements, Journal of Biomedical Materials Research Part B: Applied Biomaterials: An Official Journal of The Society for Biomaterials, The Japanese Society for Biomaterials, and The Australian Society for Biomaterials and the Korean Society for Biomaterials 84 (2008) 375–385.
[48] J Luo, FJ Martinez-Casado, O Balmes, J Yang, C Persson, H Engqvist, W Xia, In Situ Synchrotron X-ray Diffraction Analysis of the Setting Process of Brushite Cement: Reaction and Crystal Growth, ACS Appl Mater Interfaces 9 (2017) 36392–36399.
[49] P Frayssinet, L Gineste, P Conte, J Fages, N. Rouquet, Short-term implantation effects of a DCPD-based calcium phosphate cement, Biomaterials 19 (1998) 971–977.
[50] M. Bohner, Reactivity of calcium phosphate cements, Journal of Materials Chemistry 17 (2007) 3980–3986.
[51] R O'Neill, H McCarthy, E Montufar, M-P Ginebra, DI Wilson, A Lennon, N. Dunne, Critical review: Injectability of calcium phosphate pastes and cements, Acta biomaterialia 50 (2017) 1–19.
[52] J Barralet, L Grover, U. Gbureck, Ionic modification of calcium phosphate cement viscosity. Part II: hypodermic injection and strength improvement of brushite cement, Biomaterials 25 (2004) 2197–2203.

[53] S Pina, PMC Torres, JMF. Ferreira, Injectability of brushite-forming Mg-substituted and Sr-substituted α-TCP bone cements, Journal of Materials Science: Materials in Medicine 21 (2010) 431–438.
[54] K Hurle, J Weichhold, M Brueckner, U Gbureck, T Brueckner, F. Goetz-Neunhoeffer, Hydration mechanism of a calcium phosphate cement modified with phytic acid, Acta Biomaterialia 80 (2018) 378–389.
[55] L Medvecky, R Stulajterova, M Giretova, T Sopcak, Z Molcanova, K. Koval, Enzymatically hardened calcium phosphate biocement with phytic acid addition, Journal of Materials Science: Materials in Medicine 31 (2020) 54.
[56] M Bohner, J Lemaitre, TA. Ring, Effects of sulfate, pyrophosphate, and citrate ions on the physicochemical properties of cements made of β-tricalcium phosphate-phosphoric acid-water mixtures, Journal of the American Ceramic Society 79 (1996) 1427–1434.
[57] S Pina, PM Torres, F Goetz-Neunhoeffer, J Neubauer, JMF. Ferreira, Newly developed Sr-substituted α-TCP bone cements, Acta Biomaterialia 6 (2010) 928–935.
[58] S Pina, SM Olhero, S Gheduzzi, AW Miles, JMF. Ferreira, Influence of setting liquid composition and liquid-to-powder ratio on properties of a Mg-substituted calcium phosphate cement, Acta Biomaterialia 5 (2009) 1233–1240.
[59] M Bohner, U Gbureck, J. Barralet, Technological issues for the development of more efficient calcium phosphate bone cements: a critical assessment, Biomaterials 26 (2005) 6423–6429.
[60] JH Welch, W. Gutt, High-temperature studies of the system calcium oxide–phosphorus pentoxide, Journal of the Chemical Society (Resumed) (1961) 4442–4444.
[61] RG Carrodeguas, S. De Aza, α-Tricalcium phosphate: Synthesis, properties and biomedical applications, Acta biomaterialia 7 (2011) 3536–3546.
[62] B Dickens, L Schroeder, W. Brown, Crystallographic studies of the role of Mg as a stabilizing impurity in β-Ca3 (PO4) 2. The crystal structure of pure β-Ca3 (PO4) 2, Journal of Solid State Chemistry 10 (1974) 232–248.
[63] M Yashima, A Sakai, T Kamiyama, A. Hoshikawa, Crystal structure analysis of β-tricalcium phosphate Ca3 (PO4) 2 by neutron powder diffraction, Journal of Solid State Chemistry 175 (2003) 272–277.
[64] K Yoshida, H Hyuga, N Kondo, H Kita, M Sasaki, M Mitamura, K Hashimoto, Y. Toda, Substitution model of monovalent (Li, Na, and K), divalent (Mg), and trivalent (Al) metal ions for β-tricalcium phosphate, Journal of the American Ceramic Society 89 (2006) 688–690.
[65] R Enderle, F Götz-Neunhoeffer, M Göbbels, F Müller, P. Greil, Influence of magnesium doping on the phase transformation temperature of β-TCP ceramics examined by Rietveld refinement, Biomaterials 26 (2005) 3379–3384.
[66] RD. Shannon, Revised effective ionic radii and systematic studies of interatomic distances in halides and chalcogenides, Acta crystallographica section A: crystal physics, diffraction, theoretical and general crystallography 32 (1976) 751–767.
[67] JF Sarver, MV Hoffman, FA. Hummel, Phase Equilibria and Tin-Activated Luminescence in Strontium Orthophosphate Systems, Journal of The Electrochemical Society 108 (1961) 1103–1110.
[68] S Kannan, F Goetz-Neunhoeffer, J Neubauer, JMF. Ferreira, Cosubstitution of Zinc and Strontium in β-Tricalcium Phosphate: Synthesis and Characterization, Journal of the American Ceramic Society 94 (2011) 230–235.
[69] AG. Nord, Incorporation of divalent metals in whitlockite-related beta - Ca3(PO4)2. Neues Jahrbuch fur Mineralogie, Monatshefte (1983) 489–497.
[70] N Matsumoto, K Sato, K Yoshida, K Hashimoto, Y. Toda, Preparation and characterization of β-tricalcium phosphate co-doped with monovalent and divalent antibacterial metal ions, Acta Biomaterialia 5 (2009) 3157–3164.
[71] K Spaeth, F Goetz-Neunhoeffer, K. Hurle, Cu2+ doped β-tricalcium phosphate: Solid solution limit and crystallographic characterization by rietveld refinement, Journal of Solid State Chemistry 285 (2020) 121225.
[72] S Kannan, F Goetz-Neunhoeffer, J Neubauer, JM. Ferreira, Synthesis and structure refinement of zinc-doped β-tricalcium phosphate powders, Journal of the American Ceramic Society 92 (2009) 1592–1595.
[73] N Matsumoto, K Yoshida, K Hashimoto, Y. Toda, Dissolution mechanisms of β-tricalcium phosphate doped with monovalent metal ions, Journal of the Ceramic Society of Japan 118 (2010) 451–457.
[74] K Hasimoto, K Yoshida, Y Toda, T Kanazawa, S. Udagawa, Antimicrobial properties and synthesis of tricalcium phosphate doped with alkali metal and silver ions, Phosphorus Research Bulletin 13 (2002) 123–126.
[75] S Gomes, J-M Nedelec, E Jallot, D Sheptyakov, G. Renaudin, Unexpected mechanism of Zn2+ insertion in calcium phosphate bioceramics, Chemistry of Materials 23 (2011) 3072–3085.
[76] S Pina, SI Vieira, PMC Torres, F Goetz-Neunhoeffer, J Neubauer, OAB da Cruz e Silva, EF da Cruz e Silva, JMF. Ferreira, In vitro performance assessment of new brushite-forming Zn- and ZnSr-substituted beta-TCP bone cements, Journal of biomedical materials research Part B, Applied biomaterials 94 (2010) 414–420.
[77] H Cummings, W Han, S Vahabzadeh, SF. Elsawa, Cobalt-Doped Brushite Cement: Preparation, Characterization, and In Vitro Interaction with Osteosarcoma Cells, JOM 69 (2017) 1348–1353.
[78] SI El-dek, SF Mansour, MA Ahmed, MK. Ahmed, Microstructural features of flower like Fe brushite, Progress in Natural Science: Materials International 27 (2017) 520–526.
[79] S Ding, M. Wang, Studies on synthesis and mechanism of nano-CaZn2(PO4)2 by chemical precipitation, Dyes and Pigments 76 (2008) 94–96.
[80] A Laskus, A Zgadzaj, J. Kolmas, Selenium-Enriched Brushite: A Novel Biomaterial for Potential Use in Bone Tissue Engineering, International journal of molecular sciences (2018) 19.
[81] JL Aparicio, C Rueda, A Manchon, A Ewald, U Gbureck, MH Alkhraisat, LB Jerez, EL. Cabarcos, Effect of physicochemical properties of a cement based on silicocarnotite /calcium silicate on in vitro cell adhesion and in vivo cement degradation, Biomedical Materials (Bristol, United Kingdom) (2016) 11.
[82] S Maenz, E Kunisch, M Mühlstädt, A Böhm, V Kopsch, J Bossert, RW Kinne, KD. Jandt, Enhanced mechanical properties of a novel, injectable, fiber-reinforced brushite cement, Journal of the mechanical behavior of biomedical materials 39 (2014) 328–338.
[83] J Unosson, H. Engqvist, Development of a Resorbable Calcium Phosphate Cement with Load Bearing Capacity, Bioceramics Development and Applications 04 (2016) 1000074/1–/5.
[84] ABG. Lansdown, A Pharmacological and Toxicological Profile of Silver as an Antimicrobial Agent in Medical Devices, Advances in Pharmacological Sciences 2010 (2010).
[85] C Günther, H Görls, D. Stachel, Copper(II) hydrogenphosphate, CuHPO(4), Acta crystallographica Section E 65 (2009) i85 Structure reports online.
[86] YJ No, I Holzmeister, Z Lu, S Prajapati, J Shi, U Gbureck, H. Zreiqat, Effect of Baghdadite Substitution on the Physicochemical Properties of Brushite Cements, Materials Today Chemistry 12 (2019) 1719.
[87] S Meininger, C Blum, M Schamel, JE Barralet, A Ignatius, U. Gbureck, Phytic acid as alternative setting retarder enhanced biological performance of dicalcium phosphate cement in vitro, Scientific Reports 7 (2017) 558.
[88] ML Hasan, B Kim, AR Padalhin, O Faruq, T Sultana, B-T. Lee, In vitro and in vivo evaluation of bioglass microspheres incorporated brushite cement for bone regeneration, Materials Science and Engineering: C 103 (2019) 109775.
[89] B Kruppke, A-S Wagner, M Rohnke, C Heinemann, C Kreschel, A Gebert, HP Wiesmann, S Mazurek, S Wenisch, T. Hanke, Biomaterial based treatment of osteoclastic/osteoblastic cell imbalance – Gelatin-modified calcium/strontium phosphates, Materials Science and Engineering: C 104 (2019) 109933.
[90] P. Carmeliet, Angiogenesis in health and disease, Nature Medicine 9 (2003) 653–660.
[91] HHK Xu, P Wang, L Wang, C Bao, Q Chen, MD Weir, et al., Calcium phosphate cements for bone engineering and their biological properties, Bone Research 5 (2017) 17056.
[92] R Jayasree, TSS Kumar, R Venkateswari, RP Nankar, M. Doble, Eggshell derived brushite bone cement with minimal inflammatory response and higher osteoconductive potential, Journal of Materials Science: Materials in Medicine 30 (2019) 113.
[93] U. Theuretzbacher, Accelerating resistance, inadequate antibacterial drug pipelines and international responses, International journal of antimicrobial agents 39 (2012) 295–299.
[94] JL Clement, PS. Jarrett, Antibacterial silver, Met Based Drugs 1 (1994) 467–482.
[95] MM Almoudi, AS Hussein, MI Abu Hassan, N Mohamad Zain, A systematic review on antibacterial activity of zinc against Streptococcus mutans, The Saudi Dental Journal 30 (2018) 283–291.
[96] F Zhang, M Zhou, W Gu, Z Shen, X Ma, F Lu, X Yang, Y Zheng, Z. Gou, Zinc-/copper-substituted dicalcium silicate cement: advanced biomaterials with enhanced osteogenesis and long-term antibacterial properties, Journal of Materials Chemistry B 8 (2020) 1060–1070.
[97] JP. Sterling, Silver-resistance, allergy, and blue skin: truth or urban legend? Burns 40 (2014) S19-S23.
[98] C Soundrapandian, S Datta, B. Sa, Drug-Eluting Implants for Osteomyelitis 24 (2007) 493–545.
[99] B Peter, DP Pioletti, S Laïb, B Bujoli, P Pilet, P Janvier, J Guicheux, P-Y Zambelli, J-M Bouler, O. Gauthier, Calcium phosphate drug delivery system: influence of local zoledronate release on bone implant osteointegration, Bone 36 (2005) 52–60.
[100] MP Ginebra, T Traykova, JA. Planell, Calcium phosphate cements as bone drug delivery systems: A review, Journal of Controlled Release 113 (2006) 102–110.
[101] M-P Ginebra, C Canal, M Espanol, D Pastorino, EB. Montufar, Calcium phosphate cements as drug delivery materials, Advanced Drug Delivery Reviews 64 (2012) 1090–1110.
[102] GH Lee, P Makkar, K Paul, B. Lee, Incorporation of BMP-2 loaded collagen conjugated BCP granules in calcium phosphate cement based injectable bone substitutes for improved bone regeneration, Materials Science and Engineering: C 77 (2017) 713–724.
[103] F Gunnella, E Kunisch, V Horbert, S Maenz, J Bossert, KD Jandt, F Plöger, RW. Kinne, In Vitro Release of Bioactive Bone Morphogenetic Proteins (GDF5, BB-1, and BMP-2) from a PLGA Fiber-Reinforced, Brushite-Forming Calcium Phosphate Cement, Pharmaceutics 11 (2019) 455.
[104] Z Tao, W Zhou, Y Jiang, X Wu, Z Xu, M Yang, J. Xie, Effects of strontium-modified calcium phosphate cement combined with bone morphogenetic protein-2 on osteoporotic bone defects healing in rats, Journal of Biomaterials Applications 33 (1) (2018) 3–10.
[105] S Ding, J Zhang, Y Tian, B Huang, Y Yuan, C. Liu, Magnesium modification up-regulates the bioactivity of bone morphogenetic protein-2 upon calcium phosphate cement via enhanced BMP receptor recognition and Smad signaling pathway, Colloids and Surfaces B: Biointerfaces 145 (2016) 140–151.
[106] B Huang, Y Tian, W Zhang, Y Ma, Y Yuan, C. Liu, Strontium doping promotes bioactivity of rhBMP-2 upon calcium phosphate cement via elevated recognition and expression of BMPR-IA, Colloids and Surfaces B: Biointerfaces 159 (2017) 684–695.
[107] MP Hofmann, AR Mohammed, Y Perrie, U Gbureck, JE. Barralet, High-strength resorbable brushite bone cement with controlled drug-releasing capabilities, Acta Biomaterialia 5 (2009) 43–49.